SEPARATOR DESIGN FOR USE IN HIGH GVF MULTIPHASE FLOW

A Thesis

by

DANIEL IAN CIHAK

Submitted to the Office of Graduate Studies of
Texas A&M University
in partial fulfillment of the requirements for the degree of

MASTER OF SCIENCE

August 2012

Major Subject: Mechanical Engineering

Separator Design for Use in High GVF Multiphase Flow

Copyright 2012 Daniel Ian Cihak

SEPARATOR DESIGN FOR USE IN HIGH GVF MULTIPHASE FLOW

A Thesis

by

DANIEL IAN CIHAK

Submitted to the Office of Graduate Studies of
Texas A&M University
in partial fulfillment of the requirements for the degree of

MASTER OF SCIENCE

Approved by:

Chair of Committee,	Gerald Morrison
Committee Members,	Je-Chin Han
	Robert Randall
Head of Department,	Jerald A. Caton

August 2012

Major Subject: Mechanical Engineering

ABSTRACT

Separator Design for Use in High GVF Multiphase Flow. (August 2012)

Daniel Ian Cihak, B.S., The University of Texas, Austin

Chair of Advisory Committee: Dr. Gerald Morrison

The requirement of bringing an outside coolant source to run through the seals of a multiphase pump has always been a costly endeavor. Using a separator to extract liquid from the exhaust of the pump to use as a coolant is often more expensive than providing an outside source of coolant. This research proposes a cost effective separator design which efficiently separates the liquid from gas, while maintaining a high enough residence time to remove any gas entrainment, and separates only the seal flush requirement by letting any excess liquids carryover with the gas.

Conventional multiphase separators operate by substantially decreasing the velocity of the mixture, which reduces the drag force put forth by the gasses and allows gravity to force the liquids downward. Gas-Liquid Cylindrical Cyclones (GLCCs) operate by increasing the velocity of the mixture, using radial force to separate liquids and gasses. This technique requires a smaller diameter vessel to achieve separation.

The separator in this research uses gravity as the separation force while maintaining a pipe diameter similar to the GLCC. This way, only standard pipe and pipe fittings are

used. The effectiveness of this design is measured two ways. First, efficiency is studied at varying gas volume fractions (GVFs), velocities, pressures, and pipe diameters. Second, the length of air entrainment (L_{AE}) is measured at the same varying conditions.

The efficiency and air entrainment studies provide design recommendations to accommodate seal flush requirements and size limitations. The following investigation also offers further areas of research to improve the understanding and modeling of using standard pipe and pipe fittings to create more effective design equations.

ACKNOWLEDGEMENTS

I would like to thank my advisor, Dr. Morrison, for his guidance throughout my research. I would also like to thank the rest of my committee, Dr. Je-Chin Han and Dr. Robert Randall for their support.

I would like to thank my family and friends who had to put up with 6 years of college.

I would like to thank everyone at the TurboLab, especially Abhay Patil, for giving me advice and helping me finish my research.

I would like to thank Shell for sponsoring my project, because nothing can be done for free.

NOMENCLATURE

a	Acceleration
A	Cross-Sectional Area
C_D	Coefficient of Drag
d	Distance from Separator Inlet
D	Diameter
D_s	Separator Diameter
ε	Energy Dissipation
F_D	Drag Force
F_g	Gravitational Force
g	Gravitational Constant
GVF	Gas Volume Fraction
h	Liquid Height
k	Dimensionless Constant
l_s	Standing Liquid Level
L	Length
L_{AE}	Length of Air Entrainment
ṁ	Mass Flowrate
μ	Dynamic Viscosity
P	Pressure
Φ	Frictional Pressure Loss

Q_g	Gas Volumetric Flowrate
Q_l	Liquid Volumetric Flowrate
Q_w	Water Volumetric Flowrate Exiting the Bottom of the Separator
R	Gas Constant
Re	Reynolds Number
ρ_g	Gas Density
ρ_l	Liquid Density
σ	Surface Tension
T	Temperature
τ	Residence Time
τ'	Residence Time per Liquid Height
v	Velocity
v_c	Critical Velocity
v_g	Gas Velocity
v_p	Particle Velocity
W_e	Weber Number

TABLE OF CONTENTS

Page

Page

LIST OF FIGURES

Page

Page

Page

LIST OF TABLES

Page

1. INTRODUCTION

A typical problem facing many oil and gas companies is the requirement to bring an outside coolant source to run through the seals of their pump. This requires extensive equipment and cost. This thesis proposes to develop an economical and effective separator design that extracts liquid found in the exhaust of multiphase pumps to provide seal flush liquids.

Multiphase separators are a common and an essential device used in the oil and gas industry. Their wide range of designs creates many opportunities for them to be used. The method of separation varies using gravity, centrifugal, and impingement forces. Each type of separator and their strengths and weaknesses will be discussed. Modern research focuses on the gas-liquid cylindrical cyclone (GLCC), but each type of separator excels under different conditions.

Separator effectiveness is described by its capability to remove liquid droplets from the gas stream or vice versa. In high gas volume fraction (GVF) flow, liquids cause problems because of its inability to compress. Liquid droplets exist in varying sizes and can be too small to see with a human eye. Consequently, the smaller the droplet diameter the separator can catch, the more effective the separator. Drag force works against all separators. Generally, the faster the gas is moving or the smaller the liquid

---

This thesis follows the style of the International Journal of Pressure Vessels and Piping

droplet's diameter, the drag force affect is larger than the force separating the flow. Each separator type has a method to counteract drag.

Gravity type separators are the most common type and are the most basic. Gravity separators are often found in vertical and horizontal tanks, called a vessel, drum, trap or chamber. In addition, the terms knockout, flash, or compression are adjectives added before the preceding terminology to completely describe the conventional separator, i.e. knockout drum or flash trap. These separators work by making the resultant drag force from the gas particles lower than the gravitational force of the liquid particles, causing the liquid in the tank to fall and the gas to rise. To do this, the cross sectional area of the vessel is increased by a large factor over the inlet cross sectional area, decreasing velocity and the drag force, allowing the liquid to settle to the bottom of the tank[1].

Vertical separators, as show in Figure 1.1, use three separation stages. First, multiphase flow travels from the inlet and hits an inlet diverter. This causes a sudden change in momentum resulting in the largest percentage of separation. Second, gas and entrained liquid travel up through the gravity settling section, allowing liquid droplets "greater than 100 μm" to collect and fall to the liquid collection section. Lastly, the gas and liquid droplets less than 100 μm are pushed through a mist extractor where most of the remaining liquid is impinged, pooled, and forced down into the gravity settling section[1].

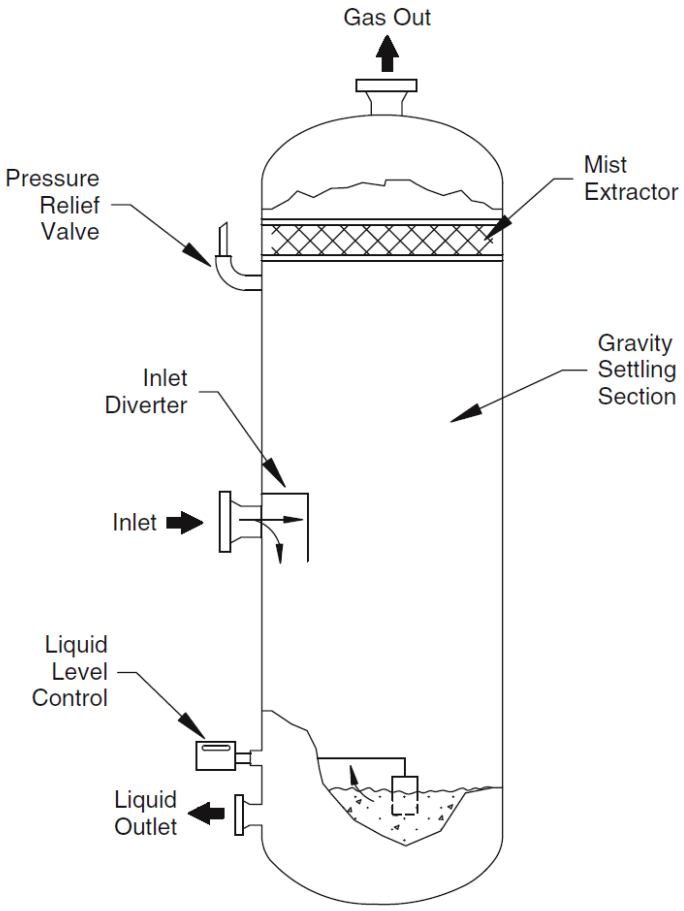

Figure 1.1. Vertical Separator[1].

The vertical separator uses two control systems, pressure regulation and liquid level control. The pressure control valve sets the pressure inside the pressure vessel. From gas properties, the higher the pressure inside the separator, the lower the gas velocity. This results in lower drag forces and higher separation between liquid and gas particles[1].

The liquid level control valve maintains the liquid level for two purposes. The first is to maximize the residence time of the liquid, which is defined by the average time a liquid particle exists in the liquid collection section before leaving the exit. This allows more time for the entrained gas to escape from the liquid collection system, resulting in more complete separation at the liquid exit. The second reason is to adjust for varying liquid loads. If the liquid's volumetric flowrate is increased, the liquid exit control valve opens to allow more liquid to leave so that the vessel does not become flooded, decreasing the separation effectiveness. If the liquid's volumetric flowrate is decreased, the valve closes to restrict the amount of liquid leaving. This prevents a case where all the liquid is drained, allowing gas to flow through the liquid exit[1].

Vertical separators have certain advantages. They are well situated for low to intermediate GVFs in multiphase flow as well as liquid surges. With its false bottom, vertical separators are useful in handling solids, including sands and other sediments. The bottom can be opened for easy removal of sands and other particles that would have eroding effects on piping and other machinery after the separator. From its verticality, this separator saves on floor space, which depending on its application and operation area, could be valuable to the operator. However, vertical separators are known to be the most expensive and have the highest cost per separation[1].

Horizontal separators are another type of gravity separator. They are based on the same flow path principles and have the same instrumentation as vertical separators

(Figure 1.2). The biggest difference is the surface area of the liquid. This allows the horizontal separator to be most effective at high GVF but less effective over the low to intermediate range, where the vertical separators excel[1].

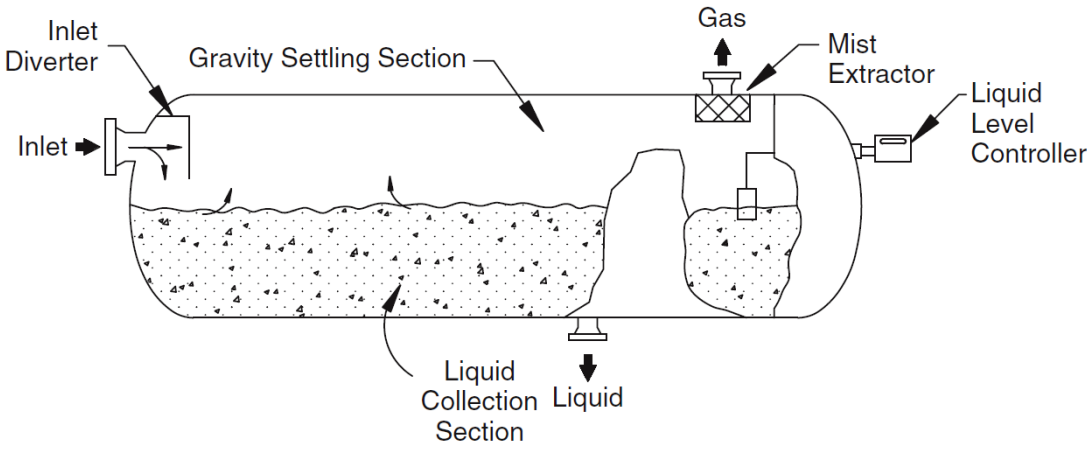

Figure 1.2. Horizontal Separator[1].

Horizontal separator advantages over vertical separators include its size and ability to handle foaming crude. If floor space is widely available, then horizontal separators offer a cheaper option for separation than vertical separators. Also, with its large liquid surface area, horizontal separators are ideal for handling a three phase separation. It shares in common with the vertical separation its residence time[1].

Centrifugal type separators use radial forces instead of gravity to force liquid downward and gas upward. The centrifugal force can be 5 to 2500 greater that of the gravitational force depending on the design. The flow uses double vortices, where the

gas is forced downward on the wall, and then spirals upward in the center, causing the tangential velocity in the separator to reach values several times that of the inlet[1]. The centrifugal force causes the denser fluid to migrate to the outside of the vessel and the less dense fluid towards the middle. Drag force does not work the same way in centrifugal separators as they do in gravity separators. Drag force in gravity separators depend on the fluid being mixed. Centrifugal separators create quick separation, negating any significant drag force that the gas would provide. This requires the tangential velocity of the mixture to be as high as possible, which is opposite of the gravitational separators[2].

Gas Liquid Cylindrical Cyclone (GLCC) is the most common type of centrifugal separator as pictured in Figure 1.3. The multiphase flow travels through the inclined tangential inlet, gas leaves through the gas outlet at the top, and liquid exits through the liquid outlet at the bottom[2]. The sensors attached to the GLCC are simpler than the two gravity separators. This gives the GLCC some advantages over the gravity separators, including having no moving parts, low maintenance, compact, and inexpensive. However, because of its simplicity, the GLCC suffers in terms of not being able to handle varying flowrates and having a low residence time[1]. Current research is trying to increase the flowrate range.

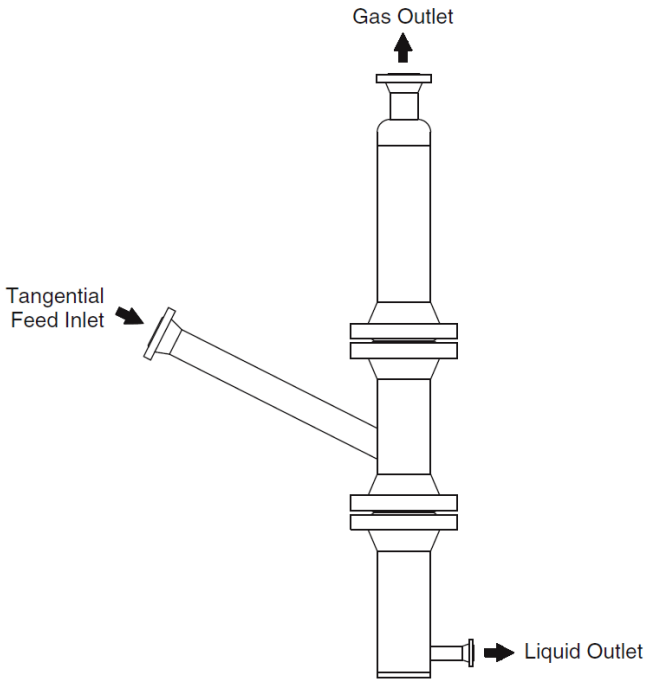

Figure 1.3. Gas-Liquid Cylindrical Cyclone[1].

Impingement type separators are used more specifically to catch small diameter droplets. The use of vanes, wires, or other methods causes water to pool, coalescing into large drops, and falling into the liquid collection region. This is accomplished by routing the mixture along a tortuous path. The mixture bumps into the vanes, causing liquid to stick to the walls. Eventually enough liquid will pool and its gravitational force will be greater than its drag force, resulting in the liquid falling down to where the other liquid is collected[2].

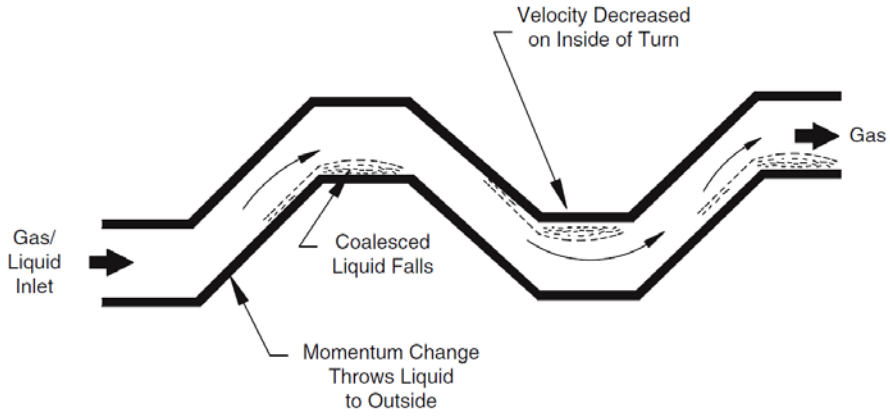

Figure 1.4. Vane Mist Extractor[1].

This type of separator needs to be installed in vessels with large diameters, specifically gravity separators or exhaust stacks. They are used to remove any liquids from the gas stream at the expense of a pressure drop. The correct mist extractor design for an application depends on cost, cross-sectional area, flow conditions, and acceptable pressure drop[1].

The goal of this project is to design a cheap, efficient separator for high GVF flows. The purpose is to recirculate the liquid used by multiphase pumps for seal flush and pump sealing when the inlet stream is solely gas, eliminating the need for an auxiliary external liquid supply. The separator described in this thesis will be different than those previously mentioned. Although it will fall under the gravity separator category, it shares many traits with the centrifugal category as well. Gravity separators require a pressure vessel for separation, while this separator will use standard pipe to operate,

similar to the GLCC, to reduce cost. A control valve placed at the water exit will control the water flowrate, in turn reducing the concern of the low residence time. By conducting the separation at the high pressure exiting the pump, the liquid and vapor mixture will have lower velocities, creating better separating conditions.

Most separators are designed to be nearly 100% effective over a wide range of operations; however, that is not the goal for the current separator. This separator theoretically needs to be 100% effective at 100% GVF inlet conditions to the pump for an infinite amount of time. This is because the same fluid can be used over and over again since the output of the pump will have at least the minimum amount of fluid needed for continued operation. If efficiencies dip below 100% at the preceding conditions, the liquid level in the separator will decrease proportionally to the efficiency deficit. Concluding, the separator needs to efficient enough so that during periods of 100% GVF inlet conditions the separator does not lose all of its standing liquid level during a finite time period.

At lower GVF values, some carryover is acceptable since new fluid is introduced at the pump entrance. The separator must be able to supply the minimum liquid required for safe pump operation. Any additional liquid in the mixture stream can be flushed downstream. While other separators want to avoid overflow, this separator will not need to retain all the liquid past its requirement set by the seal flush and pump sealing requirements.

2. LITERATURE REVIEW

Most of the current research on separators is on the emerging GLCC design. Kouba[3] and Wang[4] provide details on the basic function and design of the GLCC. This includes design parameters and critical flow equations. Chirinos[5] details the process which carryover occurs. Mohan[6] created a control system which allows the GLCC to function similar to a gravity separator.

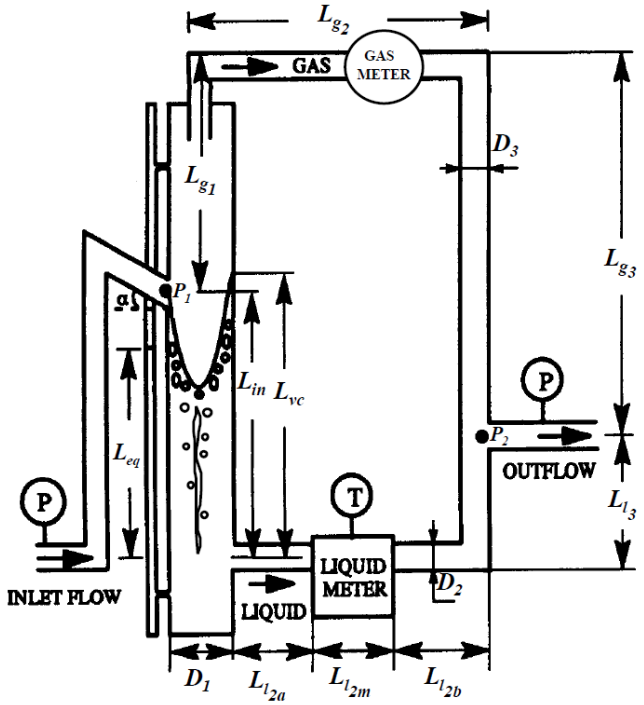

Figure 2.1. Gas Liquid Cylindrical Cyclone with Nomenclature[3].

Kouba[3] studied the performance of GLCCs and developed a model that describes its flow behavior (Figure 2.1). He found that placing the inlet inclination angle at -27 degrees from the horizontal plane produces the optimum angle for performance since the angle causes the swirl to pass beneath the inlet.

Kouba also modeled the onset to annular mist flow. This represented the minimum gas velocity for liquid carryover(2.1). To prevent carryover, the velocity of the flow needs to be less than the critical velocity. The Weber number (W_e) describes the droplet size, where large droplets represent higher numbers, such as W_e=20, while fine droplets represent smaller Weber numbers, such as W_e=7. The critical velocity will decrease with decreasing droplet size.

$$L_{eq} = \frac{\Phi_l - \Phi_g - \rho_l * g * L_{l_3} - \rho_g * g * (L_{in} + L_{g_1} - L_{g_3})}{g * (\rho_l - \rho_g) - \left(\frac{\rho_l * v_{l_1}^2 * f_{l_1}}{2 * D_1}\right)} \tag{2.1}$$

Kouba also modeled the onset to annular mist flow. This represented the minimum gas velocity for liquid carryover(2.2). The Weber number (W_e) describes the droplet size, where large droplets represent higher numbers, such as W_e=20, while fine droplets represent smaller Weber numbers, such as W_e=7. The critical velocity will decrease with decreasing droplet size.

$$v_{crit} = .6812 * \left(\sigma * W_e * \frac{\rho_l - \rho_g}{\rho_g^2}\right)^{.25} \tag{2.2}$$

Wang[4] studied the use of GLCC in wet gas applications, or a GOR (gas-oil-ratio) of 90% (by volume) and higher. High GOR is not ideal for GLCCs because of the tendency to form small liquid droplets. Wang uses the mist flow velocity v_{crit} to find the smallest gas velocity to cause liquid carryover(2.1) as described by Kouba.

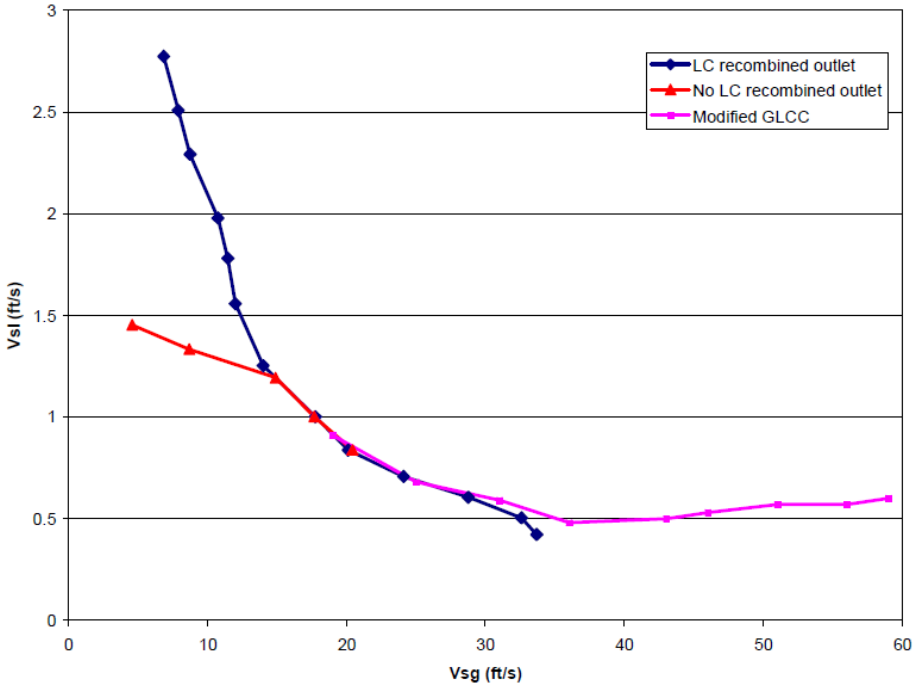

Figure 2.2. Operation Envelope for Liquid Carry-Over[4].

Wang found that unmodified GLCC liquid carryover starts at a superficial gas velocity of 20 ft/s. The superficial velocity considers only axial values and not tangential values. With a liquid level controller, described as a recombined outlet, liquid carryover doesn't start until 33 ft/s. Wang compares the condition for carryover using

the superficial liquid and gas velocities with an unmodified, a recombined outlet, and a modified GLCC as shown in Figure 2.2. The modified GLCC uses a liquid film extractor to catch liquid separated by drag forces from the liquid vortex.

Wang also recommends designs for creating an optimal GLCC while operating in wet gas conditions. First, the GLCC diameter is determined by making the gas velocity in the GLCC 2-3 times that of the critical velocity, but keeping the liquid superficial velocity lower than 0.5 ft/s. Next, he recommends an inlet inclination angle between -20 and -30 degrees with an inlet length 10 times that of the diameter.

Chirinos[5] studied the effect of liquid carry-over in GLCC separators. He first defines the operation envelope as "the initiation of liquid entrainment into the discharged gas stream at the top of the cylindrical cyclone." Chirinos found at low GVF, liquid carry-over can occur easily while at churn conditions. At high GVF, flow conditions must go beyond the operation envelope by a significant margin for liquid carry-over to exist while at annular flow conditions.

Mohan[6] created a passive control system for GLCCs. This would allow GLCCs to operate like common gravity separators. Mohan found that the equilibrium level for liquid is most influenced by the liquid flowrate, and the pressure is most influenced by the gas flowrate. This allows GLCCs to control these parameters independently at the liquid and gas outlets. However, these relationships are not as pronounced when lower

friction losses exist, which is caused by significant pressure drop in the liquid or gas collection leg at higher gas flowrates. At these conditions, active control systems are needed. Mohan experimentally found the operation envelope caused by liquid carryover. The new passive control system improves efficiency when liquid carryover exists, but only in limited flow ranges. To increase the operational envelope, Mohan reduced the pipe slot upper inlet and the sector slot lower inlet.

Stewart[1] defines the factors which affect separation, including flowrate, pressure, temperature, physical properties, and the extent of separation needed. He includes detailed descriptions on the separation methods of gravitational force, centrifugal force, and filtration. Stewart mentions secondary separation techniques, including thermal, electrostatic precipitation, adhesive separation, and absorption.

Stewart explains the differences between the horizontal, vertical, spherical, centrifugal, venture, double-barrel horizontal, filter, scrubber, and slug catcher type separators. He presents in-depth discussions on the internal components of a separator, including inlet diverters, wave breakers, defoaming plates, vortex breakers, stilling wells, sand jets, and sand drains.

In addition, Stewart recommends a 30 second to 3 minute retention time for the liquid to allow the gas and liquid to reach an equilibrium state. By using the retention

time and liquid height, Stewart developed an equation to determine the smallest liquid droplet size the separator can separate.

$$D^2 * h = \frac{\tau * Q_l}{4.713 * 10^{-8}} \quad (2.3)$$

Laleh[7] developed a CFD model that "capture[s] both macroscopic and microscopic aspects of multiphase separation phenomenon." The simulation is based on "four pilot-plant-scale two-phase separators." His results showed the most important characteristics affecting the separation of droplet sizes were the gas density and oil viscosity. Laleh found that the needed residence time is larger than that of traditional separators. Ultimately, Laleh was able to produce a way to more efficiently optimize separator design.

Kabir[8] created a model of two-phase flow in vertical wells. Kabir used pressure gradient estimations to model bubble/slug flow transition, transition to dispersed bubbly flow, slug/churn flow, and transition to annular flow. He used "an iterative finite-difference algorithm" to model each flow regime. The results are consistent with other models when flow consists mostly of single-phase, bubbly and slug flow. When the flow is churn or annular, the model performs better than existing models.

Taitel[9] modeled flow pattern transitions for steady two phase flow in vertical tubes. Bubble flow is defined as uniformly distributed gas bubbles in a continuous liquid solution. Slug flow is defined as large, bullet-shaped gas bubbles that extend the length

of the pipe diameter with a continuous liquid solution between bubbles, often having discreet gas bubbles in the liquid solution. Churn flow is defined as more chaotic than slug flow and does not have the same bullet-shaped bubbles. However, gas bubbles are elongated and liquid continuity is not always present, especially in high local gas concentrations. Annular flow is defined as a continuous gas solution, with liquid drops entrained in the gas flow. The liquid forms a thin film on the edges on the pipe. Taitel notes that the current transition boundaries are based with little theoretical foundation. However, their models for transition flow show good agreement with experimental data.

Stewart[10] describes an alternative approach to demisting gas and liquid flow streams. This device is called an axial flow cyclone, and it would be used instead of vane or wire demisters. Advantages over the vane or wire mesh includes being able to handle higher gas loads, have a smaller pressure drop, and decrease the weight of the separation system. Stewart begins by defining the maximum liquid droplet size that can enter the scrubber, or Hinze equation(2.4). Where σ is the surface tension, ρ is density, ε is energy dissipation, and k is a dimensionless constant.

$$D_{max} = k * \frac{\sigma^{0.6}}{\rho^{0.6} * \varepsilon^{0.4}} \tag{2.4}$$

Stewart explains that the axial flow cyclone scrubber is not best suited for all applications. He compares four separation techniques and rates them from worst (4) to best (1). Axial flow cyclones are best suited for situations where the smallest pressure drop is needed.

Table 2.1. Performance Criteria for Different Demisting Devices[10]

DEVICE	Multicyclone	Vane Pack	Axial Flow Cyclone	Mesh Pad
Turndown	1	4	2	3
Capacity/Unit Area (Low Pressure)	3	1	2	4
Capacity/Unit Area (High Pressure)	2	3	1	4
Pressure Drop	4	2	3	1
Solids Handling	1	3	2	4
Drop Size Removal @ atmosphere (μm)	4	10	7	10

3. THEORY

3.1. Velocity Calculation

3.1.1. Volumetric Flowrate

There are two fluid types which exist in a separator; liquid and vapor. A way to measure the flowrate of both fluid types is to use volumetric flowrate. Volumetric flowrate is defined two ways. The first is by the area multiplied by the velocity as shown in equation(3.1) or as the density divided into the mass flowrate in equation(3.2). Volumetric flowrate will not be conserved at varying densities, meaning liquids will have a conservation of volumetric flowrate if the temperature is constant, while for vapors, Q will vary with temperature and pressure.

$$Q = A * v \tag{3.1}$$

$$Q = \frac{\dot{m}}{\rho} \tag{3.2}$$

Area is found by using the inside diameter of the given cross section as shown in equation(3.3). The diameter is represented by the diameter of the projected plane.

$$A = \frac{\pi}{4} * D^2 \tag{3.3}$$

Volumetric flowrate is useful in multiphase flows. Q can be used separately to identify individual fluids, and later added together to represent the combination of fluids. This gives rise to the term gas volume fraction (GVF) which is the ratio of gas volumetric flowrate to the total volumetric flowrate(3.4). GVF will not be conserved

through different cross sectional areas, but it a very important tool for describing inlet conditions.

$$GVF = \frac{Q_{gas}}{Q_{gas} + Q_{liquid}} \tag{3.4}$$

3.1.2. Ideal Gas Law

Since the gas used in this study is air, gas properties can be modeled by using the ideal gas law. As equation(3.5) shows, the density of the gas is directly dependent on its pressure and temperature.

$$P = \rho_g * R * T \tag{3.5}$$

Since temperature is largely kept constant, pressure is the defining parameter. Density is a variable that changes in gas, but stays constant in liquids at varying pressures, meaning the volumetric flowrate is constant in liquids but will vary in gasses at different pressures.

3.1.3. Conservation of Mass

Despite the importance of volumetric flowrate, mass flowrate is the important constant parameter throughout the separation process. Mass flowrate at the inlet condition is found by knowing the volumetric flowrate, pressure, temperature, and gas constant. Equation(3.6) is just a recombination of equation(3.2) and equation(3.5) .

$$\dot{m} = \frac{Q * P}{R * T} = \rho * Q \tag{3.6}$$

To determine the gas velocity inside the separator, equation(3.1) and equation(3.6) are combined to form equation(3.7) , which is dependent on the pressure, temperature, gas constant, mass flowrate, and the diameter of the pipe.

$$v = \frac{4 * \dot{m} * R * T}{\pi * P * D_s^2} \tag{3.7}$$

Liquid mass flowrate is ignored because it is assumed the liquid is separated from the air and falls to the bottom of the separator. Velocity of the gas is a critical design factor due to its importance in drag force. Its inverse relationship with pressure is one of the primary focuses of this research.

3.2. Finite Element Analysis

3.2.1. Liquid Droplet Approximation

Since this separator utilizes only gravitational force to remove the liquid from the gas, a Finite Element Analysis (F.E.A) is a useful tool to view all the forces that act with or against gravity. A liquid droplet, due to its surface tension, can be viewed as a sphere at a small scale as shown in Figure 3.1, forces acting on a single droplet can be reduced to a gravitational force downward and a drag force upward.

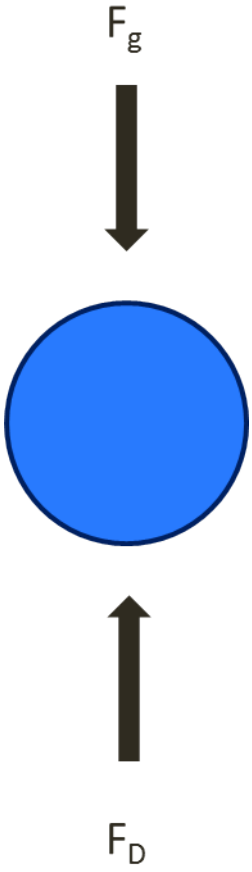

Figure 3.1. Forces on a Liquid Droplet

3.2.2. Drag Force Calculation

This process is used to determine the critical diameters and velocities for a given liquid droplet. When the drag and gravitational forces are equal, the separator is operating at its critical condition where increasing the gas flow will cause liquid to carry over out of the separator with the gas. To evaluate the, the drag force is set equal to gravitational force. By setting the diameter, one can find the effective velocity can be determined and vice versa. The gravitational force will remain constant for any mass,

but the drag force will vary. The gravitational force is represented in equation(3.8). The gravitational constant is -9.81 m/s^2.

$$F_g = \frac{\pi}{6} * D_d^3 * \rho_l * g \tag{3.8}$$

Drag force is highly nonlinear and cannot be captured in a single equation without some approximation. This is because of its relation with coefficient of drag as shown in equation(3.9).

$$F_D = \frac{\pi}{8} * C_D * \rho_g * v^2 * D_d^2 \tag{3.9}$$

The coefficient of drag is a dimensionless unit that has a direct correspondence to the Reynolds Number, another dimensionless unit. This relationship presented in (3.10) varies for different geometries and Reynolds Numbers.

$$Re = \frac{\rho_g * v * D_d}{\mu_g} \tag{3.10}$$

For Re less than 2, Stoke's Law approximation is used as described in equation (3.11). Because of the low gas mass flowrate, the coefficient of drag experiences a linear inverse relationship with Reynolds Number.

$$C_D = \frac{24}{Re} \tag{3.11}$$

Combining equations(3.9)(3.10)(3.11) , the drag force is reduced to a single equation, as seen in equation(3.12). Despite the fact the drag force is being characterized as a function of the velocity and diameter squared, flow in the laminar region loses a square on both parameters.

$$F_D = 3 * \pi * \mu_g * v * D_d \tag{3.12}$$

Setting the drag force equal to the gravitational force reveals an equation to find the velocity at which there is a net zero force acting on a particle(3.13). This produces good baseline results if no other outside forces act on the particle. Figure 3.2 shows the relationship between the effective diameter and gas velocity using a liquid density of 999 kg/m^3 and a gas viscosity of 0.183 cP.

$$v = \frac{-g * D_d^2 * \rho_l}{18 * \mu_g} \tag{3.13}$$

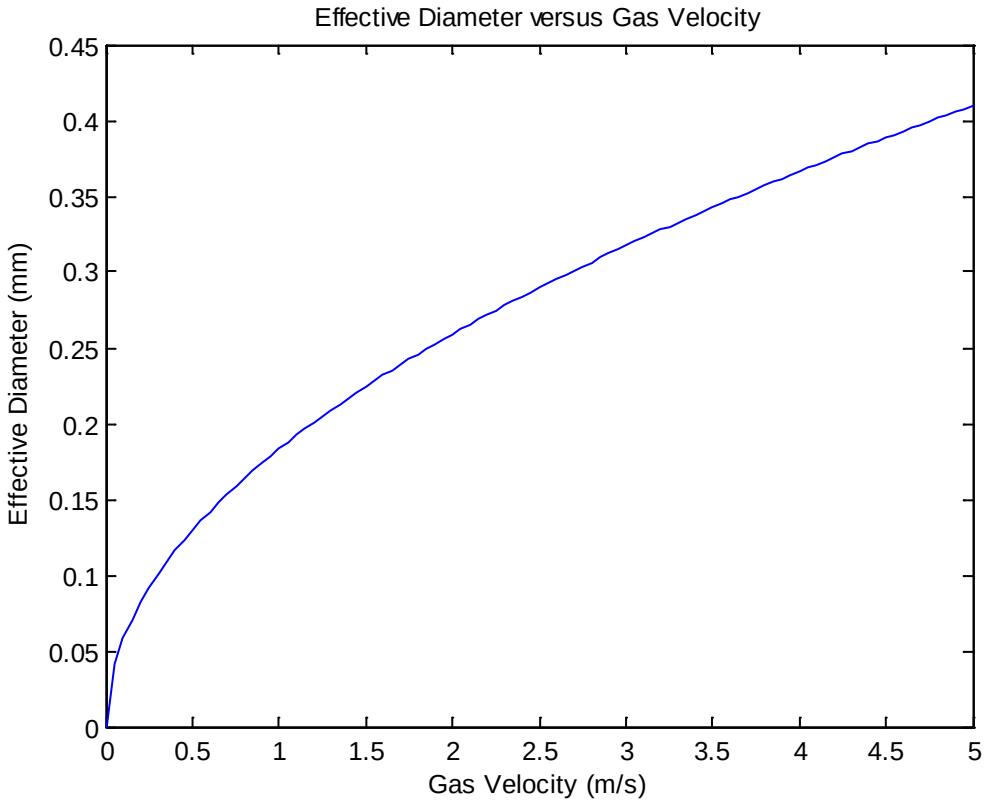

Figure 3.2. Relationship Between Gas Velocity and Particle Diameter

3.2.3. Second Law of Motion

The previous equations assume only drag and gravitational forces acting on the particle and is a good representation of a tee pipe fitting. However, if a particle reaches the standing water before the resultant force had time to decelerate the downward velocity, the surface tension of the water would outweigh both the drag and gravitational forces. The wye pipe fitting uses this technique, causing the water to have an initial negative velocity in the downward direction, as opposed to the tee, which has no downward velocity component.

A simplified model of this approach will be demonstrated to determine worst case scenario liquid collection. By keeping the largest force on the droplet constant, which turns out to be the initial force in the separator, the model will not overestimate the separator's ability to remove liquid from the mixture. This is needed prove the wye's theoretical advantage without making any assumptions which could potentially increase the wye's true effectiveness. Using the particle as the stationary frame of reference, the drag force calculation can be reassembled. The velocity will have two components: one from the gas and one from the liquid particle(3.14).

$$v = v_g - v_p \tag{3.14}$$

By using a larger velocity, the initial drag force seen on the liquid particle is actually greater than the stationary particle. However, Newton's second law of motion reveals that even though the liquid particle experiences larger forces, its initial negative velocity causes it to initially travel downward(3.15).

$$F_{net} = \frac{\pi}{6} * D_d^3 * \rho_l * a \tag{3.15}$$

The simplification of this model begins here where normally as the particle decelerates, the drag force acting on the particle reduces, causing the acceleration to slow. This model will simplify the process and assume the initial acceleration is constant throughout the process. Using geometry, the relationship between the particle velocity and the gas velocity can be determined(3.16).

$$v_p = -v_g * \cos 45 \tag{3.16}$$

Using the equations of motion and a final velocity equal to 0, the relationship between the factors distance traveled, gas velocity, and particle diameter can be arranged(3.17).

$$d = \frac{v_g^2 * D_d^2 * \rho_l}{72 * \mu_g * v_g * (1 + \cos 45) + 4 * g * D_d^2 * \rho_l} \tag{3.17}$$

Equation (3.17) adds a new design parameter, d, distance traveled. The distance traveled represents the length a specific particle travels in the separator before it loses its initial negative velocity. The distance traveled is expressed as a negative because the positive direction is considered upwards. Figure 3.3 shows the relationship between the gas velocity, the distance the particle can travel in the separator, and the minimum diameter particle which is able to move the specified distance at the specified gas velocity. A liquid density of 999 kg/m^3 and a gas viscosity is 0.183 cP is used for both the tee and wye pipe fittings.

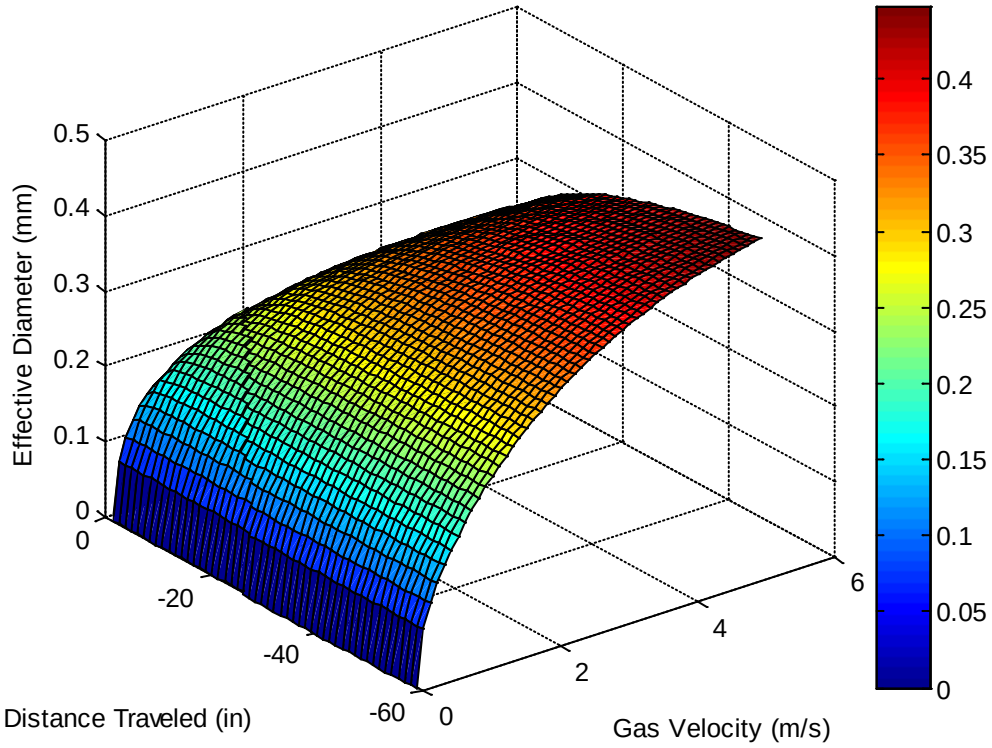

Figure 3.3. Comparison of the Gas Velocity, Effective Particle Diameter, and Distance Traveled

To better compare the advantages of the wye pipe fitting, Table 3.1 compares how the minimum diameter particle, defined by the tee pipe fitting constraints, performs in the wye pipe fitting. As expected, the wye is able to push the particles further, increasing its chance to collect them.

Table 3.1. Comparison of the Tee and Wye Pipe Fittings

Velocity (m/s)	Diameter (mm)	d (in)	
		Tee	Wye
0	0	0	0
1	0.183184	0	-1.4189
2	0.259062	0	-5.6756
3	0.317285	0	-12.7701
4	0.366369	0	-22.7024
5	0.409613	0	-35.4725

3.3. Air Entrainment

Despite the advantages of the wye pipe fitting, the increase in momentum of the collected particles has one distinct disadvantage when compared to the tee. An increase in gas entrainment is expected. Gas entrainment is described as the creation of tiny gas bubbles in the liquid caused by the collisions of the standing water level and falling liquid stream. The more turbulent the collision, the more gas entrainment that will be seen.

To remove the gas entrainment from the standing liquid level, there needs to be a sufficient time period for the liquid to exist in the separator. The average time the liquid exists is known as the residence time. The residence time is found in equation(3.18).

$$\tau = \frac{\pi * D_s^2 * h}{4 * Q_w} \tag{3.18}$$

There are a few options to increase residence time and remove gas entrainment. Decreasing the liquid volumetric flowrate, increasing the standing liquid level, or

increasing the separator pipe diameter are all viable ways to increase the residence time, but are often constrained by physical limitations.

4. EXPERIMENTAL FACILITY

This chapter describes the experimental facility found at the Turbomachinery Laboratory of Texas A&M University and its capabilities to test multiphase flow at varying flow conditions. To simulate multiphase flow, air and water are controlled at the separator inlet.

Section 4.1 focuses on the hardware surrounding the separator. This includes how water and air are stored, transported, and measured. Section 4.2 focuses on the separator assembly. Section 4.3 describes the instrumentation and section 4.4 focuses on the data acquisition.

4.1. Experimental Hardware

This section will describe how the water and air are stored, transported, and combined. Figure 4.1 illustrates the infrastructure of the laboratory. The water flow loop operates using a 135 GPM centrifugal pump which draws water from a 5000 gallon reservoir. The flow is controlled by two electro-pneumatic placed before two water flowmeters. The air flow loop consists of a series of oil free air compressors and a common storage tank, which is not pictured. The flow is measured by two flowmeters and controlled by a single electro-pneumatic valve. The air and water are combined before the separator inlet at the desired gas volume fraction. The air leaves the top of the separator and exits through the water storage tank and released to the atmosphere. The

water leaves through the bottom, passes through a flowmeter, and exits to the open atmosphere.

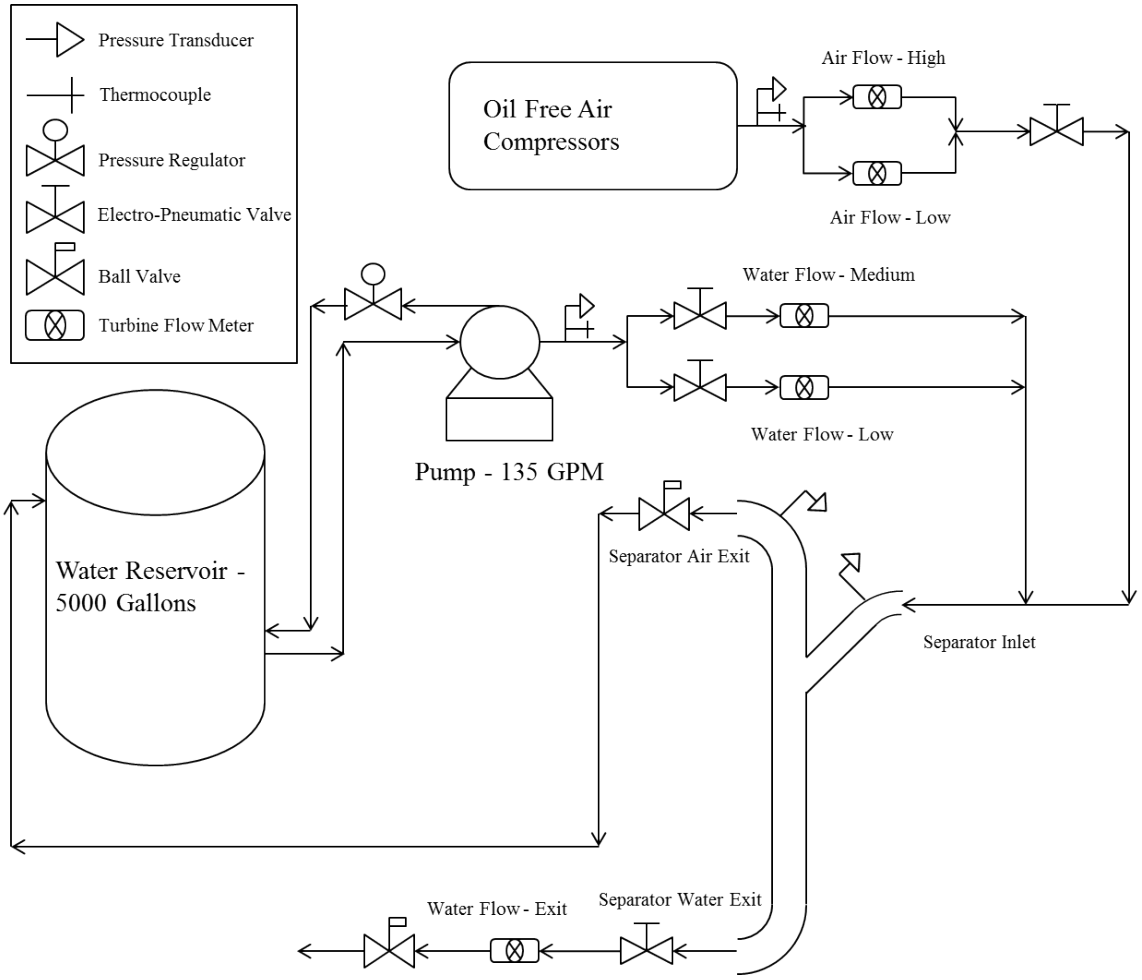

Figure 4.1. Flow Loop Diagram

Figure 4.2 and Figure 4.3 shows the water system outside the laboratory. The water is initially stored in a 5000 gallon storage tank. The water is fed through a 135 GPM centrifugal water pump, while a pressure regulator maintains a pressure level of 120 psi.

Once the water leaves the pump, it flows into the laboratory where it is controlled and measured.

Figure 4.2. Water Reservoir

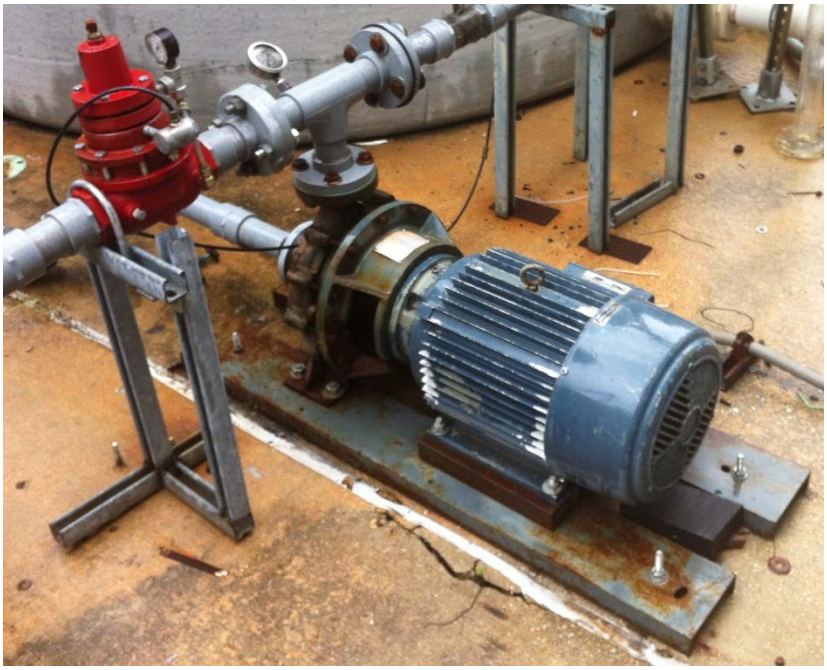

Figure 4.3. Centrifugal Pump and Pressure Regulator

Figure 4.4 shows the water control system inside the laboratory. The electro-pneumatic valves are controlled by a NI-9205 module operated by a LabVIEW. The control valves regulate the flow of water and the flowmeters measure the flow. Only the low and medium sized flowmeters are used due to the high GVF required, but even higher flowrates are available if necessary.

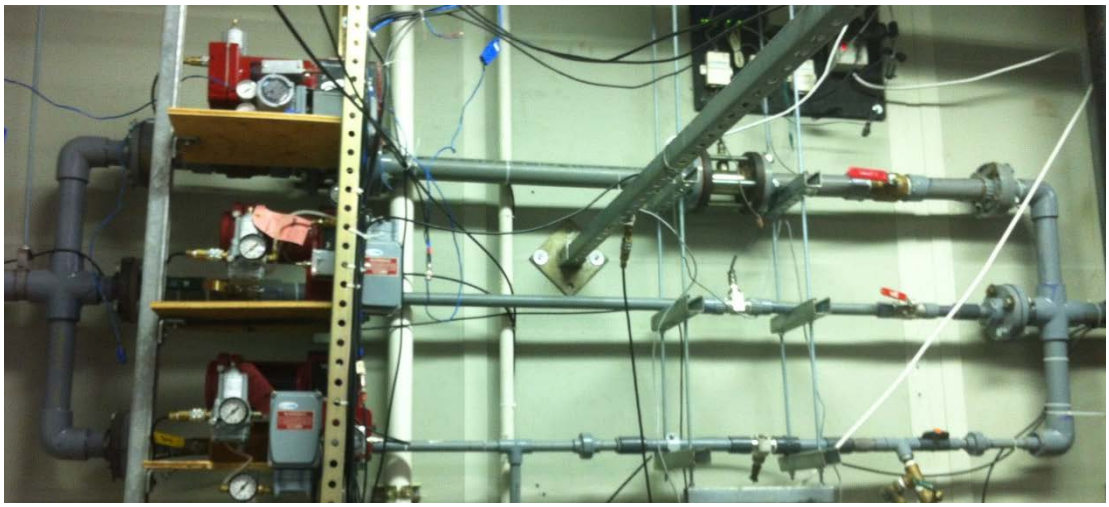

Figure 4.4. Water Manifold

Figure 4.5 and Figure 4.6 show the air control system. The oil free air compressors are responsible for pressurizing the air to 115 psi. Water is removed from the air and the air is then stored in a large tank. The air manifold is responsible for measuring and controlling air flow. Two turbine flowmeters are used to measure flowrate. An electro-pneumatic valve is used after the flowmeters to regulate the flowrate. This action is performed by a PID controller in LabVIEW.

Figure 4.5. Oil-Free Air Compressors

Figure 4.6. Air Manifold

The pressure inside a separator operating with a multiphase pump would be controlled by the ball valve on the separator exit as pictured in Figure 4.7. With the PID controller installed on the air manifold, the ball valve now the separator and mixture velocities while the air manifold sets the operating pressure. This allows the operator to use the PID controller to define the pressure and use the ball valve positioning to determine velocity. Velocity needs to be closely regulated because it is one of the important testing variables in determining the separator's efficiency.

Figure 4.7. Separator Air Exit Ball Valve

Figure 4.8 shows the electro-pneumatic valve and turbine flowmeter located at the separator water exit. The valve controls the amount of water that leaves the separator and the height of water inside the separator. It is important to maintain a minimum level of water to create a seal to keep air from exiting out the bottom of the separator. The seal, instead, forces the air to flow through the top of the separator. The flowmeter is

used to measure the liquid flow and has the same measuring range as the medium flowmeter on the water manifold.

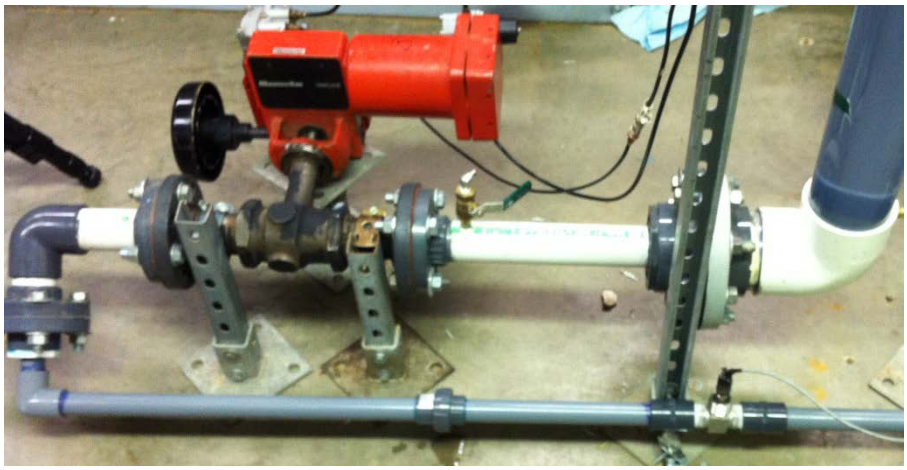

Figure 4.8. Separator Water Exit

4.2. Separator Assembly

The separator prototype is made from transparent schedule 80 PVC to provide a visual representation of liquid loss and gas entrainment as seen in Figure 4.9. By using schedule 80 PVC, the separator will be able to handle pressure up to 135 psi at room temperature conditions, which is above the supply pressure of 120 psi from both the air and water. The wye is not transparent, based on cost considerations, but the alternate tee pipe fitting is (Figure 4.10). The two pipe fittings will be compared to show which is more efficient at removing liquid from air.

Figure 4.9. 6" Separator with Wye Pipe Fitting

Figure 4.10. Tee Pipe Fitting

Two pipe diameters are tested. The 4” pipe is tested using the wye and tee pipe fittings, while the 6” pipe is tested using only the wye pipe fitting. The different size pipes show the effect of residence time against air entrainment and efficiency against water flowrate. The 6” pipe will require higher flowrates to reach the same velocities set by the 4” pipe.

The air and water are brought to the separator separately, and are combined before the separator's inlet. The air and any water carried over (not separated) leave out of the top of the separator. The water exits via the bottom of the separator and is metered and drained outside the laboratory cell as shown in Figure 4.8.

4.3. Instrumentation

To accurately study the separator's effectiveness at removing water from air for a variety of GVFs and velocities, different types of pressure transducers, differential pressure transducers, thermocouples, flowmeters, and control valves are used. The sensors are connected to a LabVIEW using data acquisition cards. The list of sensors is expressed in Table 4.1.

Table 4.1. List of Sensors

Sensor Number	Symbol	Measured Quantity	Principle	Type/Manufacturer
1	Pa	Pressure - Air Inlet	Solid State	Omega PX181B
2	Pm	Pressure - Mixture		
3	Po	Pressure - Air Outlet		
4	Tw	Temperature - Water Inlet	Peltier Effect	Omega T-Type
5	Ta	Temperature - Air Inlet		
6	Qw1	Flow - Water - Medium	Turbine Meter	Omega FTB-1425
7	Qw2	Flow - Water - Low		Omega FTB-1422
8	Qwe	Flow - Water -Exit		Omega FTB-1425
9	Qa1	Flow - Air - High		Daniel Industries/ Omega FTB-938
10	Qa2	Flow - Air - Low		Omega FTB-933
11	h	Liquid Height	Bernoulli's	Rosemount 3051

4.3.1. Turbine Flowmeters

Flowmeters operate by straightening out the flow to reduce turbulence then using the flow to spin a turbine. The turbine spins at a speed proportional to the speed of the fluid. The spin causes a magnetic field which generates a pulse of AC voltage. The output from the turbine meter is the frequency of the pulse, which is proportional to the volumetric flowrate. The utilization of the flowmeters require a straight pipe length of 10 diameters (a term denoting a length 10 times that of its cross sectional diameter) upstream and 5 diameters downstream for improved accuracy.

Figure 4.11. Turbine Flowmeter

Table 4.2 displays the turbine meters used in the experiment. Two air flowmeters are used to measure the flowrate at any one time to extend the range at which the air can be supplied. For the high air flow, the Daniel flowmeter needed to be replaced during the testing procedures. Three liquid flowmeters are used to measure the flowrate of

water. Two are used before the inlet and one at the separator exit which is shown in Figure 4.11.

Table 4.2. Flowmeters

Fluid	Range	Model	Range
Air	High	Daniel Industries	10-100 ACFM
Air	High	Omega FTB-938	8-130 ACFM
Air	Low	Omega FTB-933	2-28 ACFM
Water	Medium	Omega FTB-1425	5-50 GPM
Water	Medium	Omega FTB-1425	5-50 GPM
Water	Low	Omega FTB-1422	0.75-7.5 GPM

4.3.2. Pressure Transducers

Pressure is measured using solid state pressure transducers produced by Omega, series PX181B. The pressure transducers have an excitation of 9 to 30 VDC, output of 1 to 5 VDC, and an accuracy of .3% BFSL maximum. Table 4.3 details the pressure range at each location.

Table 4.3. Pressure Transducers

Location	Pressure Range	Error
Air Inlet	0-200 psi	0.6 psi
Separator Inlet	0-300 psi	0.9 psi
Air Outlet	0-300 psi	0.9 psi

4.3.3. Differential Pressure Transducer

The height of liquid in the separator is measured by a Rosemount 3051 differential pressure transducer shown in Figure 4.12. The differential pressure transducer measures the local gauge pressure, not absolute, between taps at the bottom and top of the separator and outputs a 4-20 mA signal. The output is proportional to the difference in pressure, which is then converted to liquid height. The conversion 1 psi to 27.68 inches of water is used. The Rosemount 3051 has an accuracy of 0.065% of the span with 0.04% Optical, a performance of 0.15% of span, and a range of 0-250 inches of water.

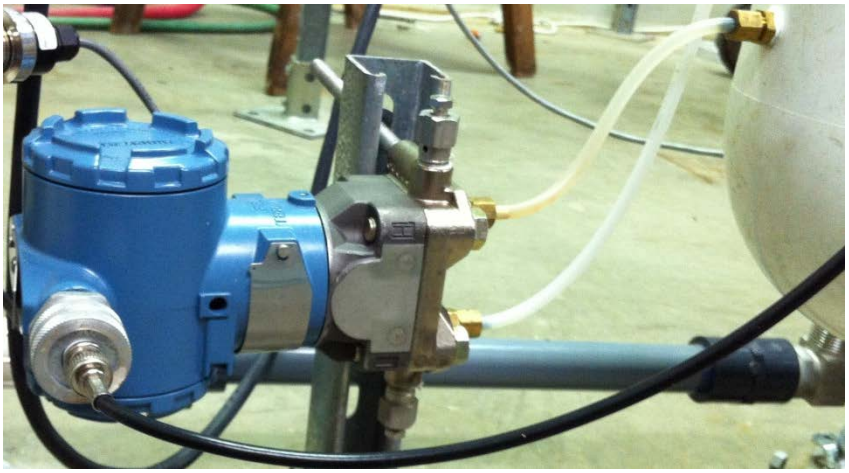

Figure 4.12. Differential Pressure Transducer

4.3.4. Thermocouples

Two Omega T-Type thermocouples are used to measure the inlet water and air conditions. The thermocouples are coupled with a NI-9213 card with built-in CJC. The error is the greater value of 1.7ºC or 0.5%.

4.3.5. Control Valves

Figure 4.13 shows a Masoneilan Camflex Rotatory Control Valves, which is electro-pneumatically controlled by a NI-9265 card. The valves use a 4-20 mA signal to control the valve to reach the desired flow conditions. A PID controller is attached to the air inlet valve to regulate the air pressure to the level set by LabVIEW.

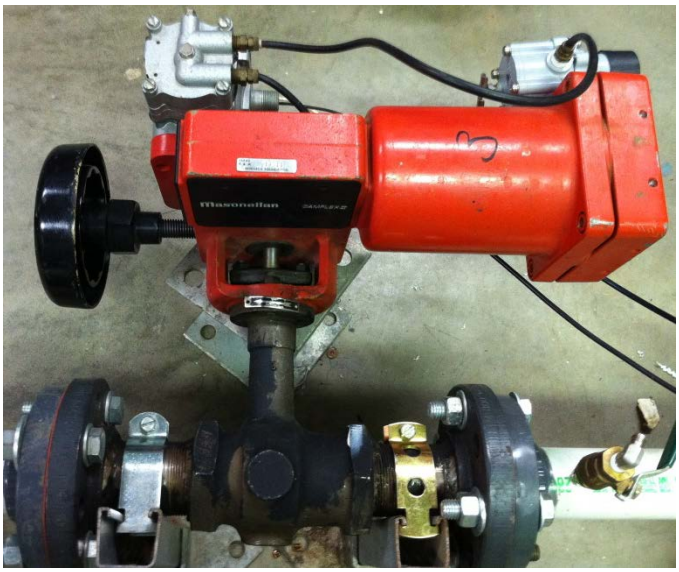

Figure 4.13. Masoneilan Control Valve

4.3.6. Video Camcorder

Figure 4.14 shows the Sony HDR-CX560V video camera used to record the level of air entrainment in the bottom half of the separator. The camera has 1920 x 1080 60p specifications and uses 64GB of memory to store video.

Figure 4.14. Video Camcorder

4.4. Data Acquisition

4.4.1. DAQ Chassis

Figure 4.15 shows the NI-9172 module chassis which stores the four NI modules connected to LabVIEW. The NI-9205 and NI-9215 modules are used to measure pressures, including from the signal from the differential pressure transducer using 10 V signal. The NI-9213 module is used to collect thermocouple data. The NI-9265 controls the Masoneilan valves with a 4-20 mA output signal.

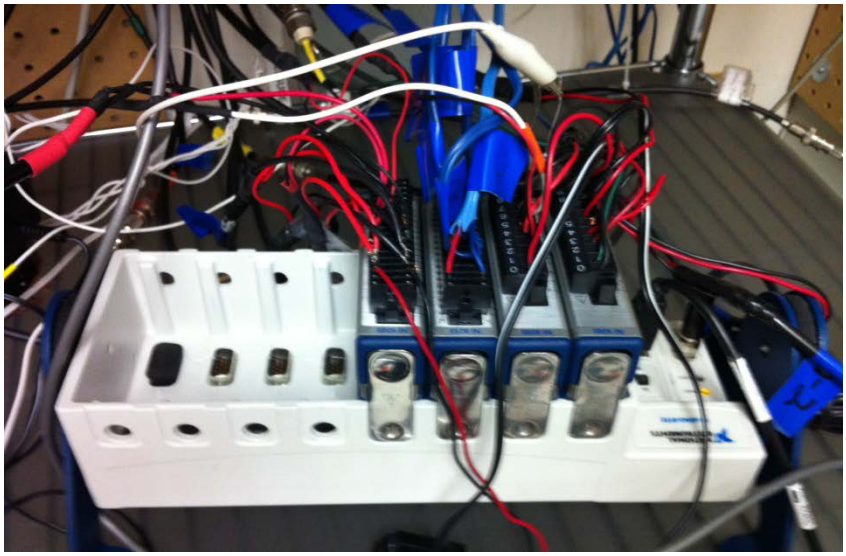

Figure 4.15. DAQ Chassis

4.4.2. LabVIEW

The sensory data is recorded and pneumatic valve set using LABVIEW 2010 as shown in Figure 4.16. The LABVIEW program has the capability to display all the pressures, temperatures, and flowrates with minimal delay. The program has the capability of reading the differential pressure transducer output and converting it to the current water level in the separator in real time. There is a manual controller that manages the valves. A PID can be turn on or off to control the mixture pressure. An LED light has been installed on the separator to inform the user when data is being saved to synchronize with a video recording device. The program is able to calculate velocity and GVF in real time and use the data to inform the user what flowrates at which the system needs to run.

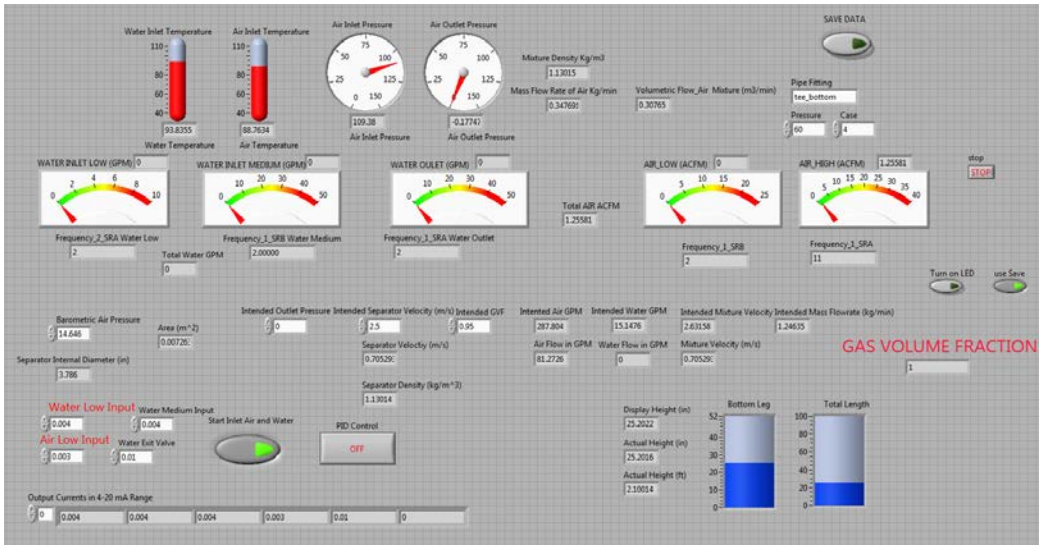

Figure 4.16. LabVIEW Program

4.4.3. PID Controller

Figure 4.17 shows the PID control in LabVIEW which controls the pressure inside the separator. Also included in the figure are the manual controls for the Masoneilan valves.

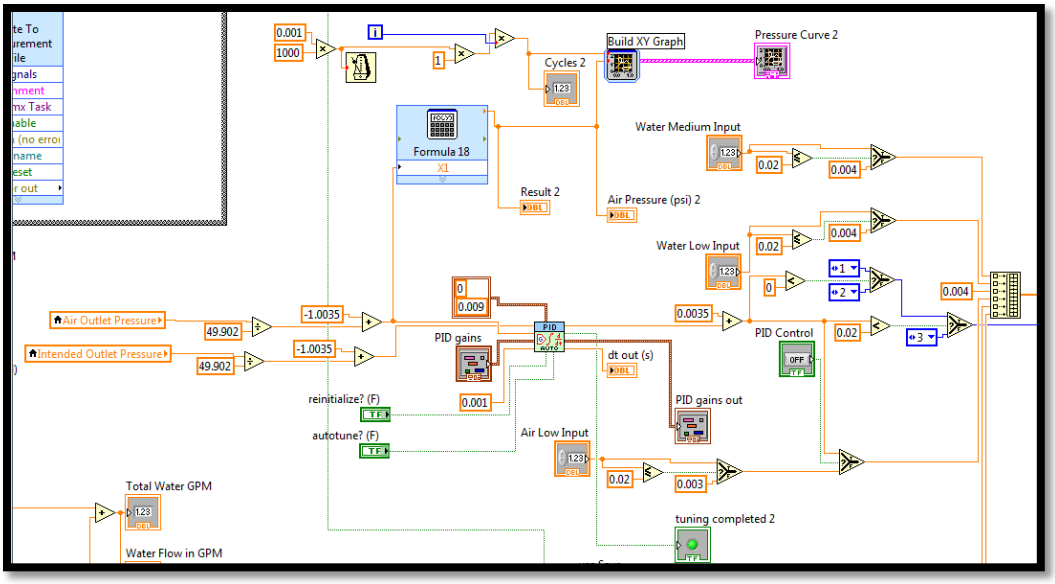

Figure 4.17. PID Controller

4.4.4. GVF and Velocity Calculation

Figure 4.18 shows the real time calculation of both GVF and separator velocity. The continuous calculation and display of the GVF and velocity are important to make sure the separator is running at the conditions set by the operator. Variations from the intended values allow the operator to make immediate corrections. The GVF and velocity are calculated for values entering the separator, often denoted as the mixture condition.

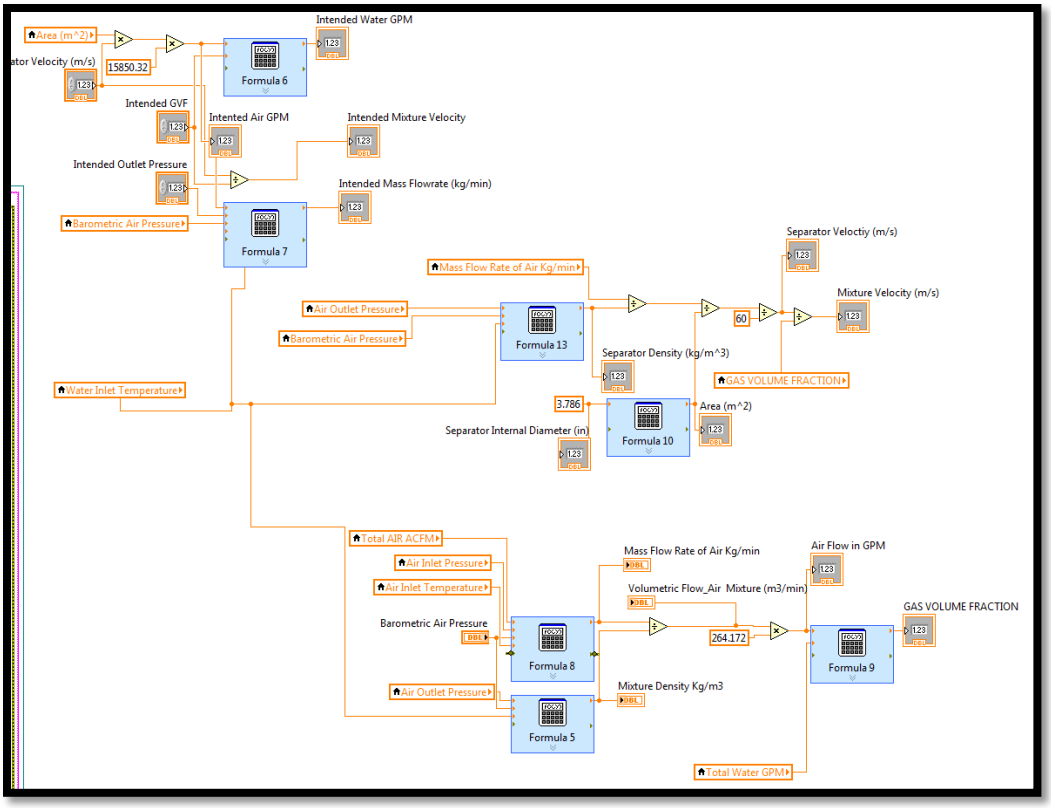

Figure 4.18. GVF and Velocity Calculation

5. RESULTS

This chapter presents the results of the study and provides an interpretation of the results. Section 5.1 focuses on efficiencies. How efficiency changes with varying volumetric flowrates, velocities, GVFs, and pipe diameters is discussed. Section 5.2 focuses on air entrainment and residence time. This section is dependent on a more visual aspect to determine the level of air entrainment than what is used to calculate efficiency.

The experiments are performed by setting the GVF, pressure, and velocity of the air and water mixture inside the separator. A hypothetical experimental table containing the three changing variables is shown in Table 5.1. These values represent the approximated values used in the study. By testing at these conditions, an understanding on how efficient the separator is and how it changes with GVF, pressure, and velocity is obtained.

Table 5.1. Test Parameters for the 4” and 6" Separators

GVF (%)	Pressure (psi)	Velocity (m/s)
90	15	0.5
	30	1.0
95	45	1.5
	60	2.0
99	75	2.5

After studying the wye pipe fitting on the 4” separator, the tee pipe fitting is installed. Table 5.1 defines the absolute parameters of the experiment, and the results compared to the wye pipe fitting. The 6” pipe is installed with the 6” wye pipe fitting to compare the effect of pipe diameter on separation and the level of air entrainment.

5.1. Efficiency Comparison Study

The efficiency tests are performed by first obtaining steady state operating conditions at the desired GVF, pressure, and velocity. The procedure, which is viewed in Figure 5.1, begins once all variables are stabilized. The water is then drained to level of 10 inches above the bottom pressure transducer tap. The exit valve is closed and the water level is allowed to rise. The experiment is stopped when the water reaches 7 inches from the bottom of the wye. This equates to a height of 45” for the 4” separator and 75” for the 6” separator.

Figure 5.1. Example of Testing Procedure

The efficiency(5.1) is measured using the linear time derivative of liquid height. This is converted to volumetric flowrate by multiply the height changer per time by its area and dividing the result by the inlet volumetric flowrate.

$$\eta = \frac{\frac{dh}{dt} * \pi * D^2}{4 * Q_i} \tag{5.1}$$

5.1.1. Water Flowrate

Water flowrate is the most important factor when comparing efficiencies. The water flowrate is determined by a combination of GVF and velocity, but is independent of

pressure. The pump on which the separator is attached will have a demand for a minimum amount of liquid to run through the mechanical seals. Independent of air velocity, GVF, or pressure, the separator needs to provide the minimum amount of liquid at any condition. Table 5.2 shows the water flowrate values for the 4" pipe fitting using the specific GVFs and velocities.

Table 5.2. Water Flowrates for the 4" Wye Fitting

Average GVF	Average Velocity (m/s)	Average Water Flowrate (GPM)	Average Efficiency (%)	Standard Deviation (%)
0.950	0.51	3.04	100.07	1.01
0.990	2.52	3.08	100.42	0.32
0.950	1.03	6.15	101.05	0.39
0.900	0.50	6.30	100.00	0.51
0.950	1.51	9.07	100.68	1.02
0.950	1.98	12.06	98.83	1.84
0.901	1.02	12.80	98.89	1.23
0.950	2.50	15.19	98.38	1.31

Figure 5.2 shows the relationship between the water supply and efficiency. Before 10 GPM, the average efficiency is close to the theoretical maximum limit of 100% at 100.4%. After 10 GPM, there seems to be a clear drop in efficiency, albeit small. At 12.4 GPM, the average efficiency dips to 98.9% and at 15.2 GPM, the efficiency finally falls to 98.4%.

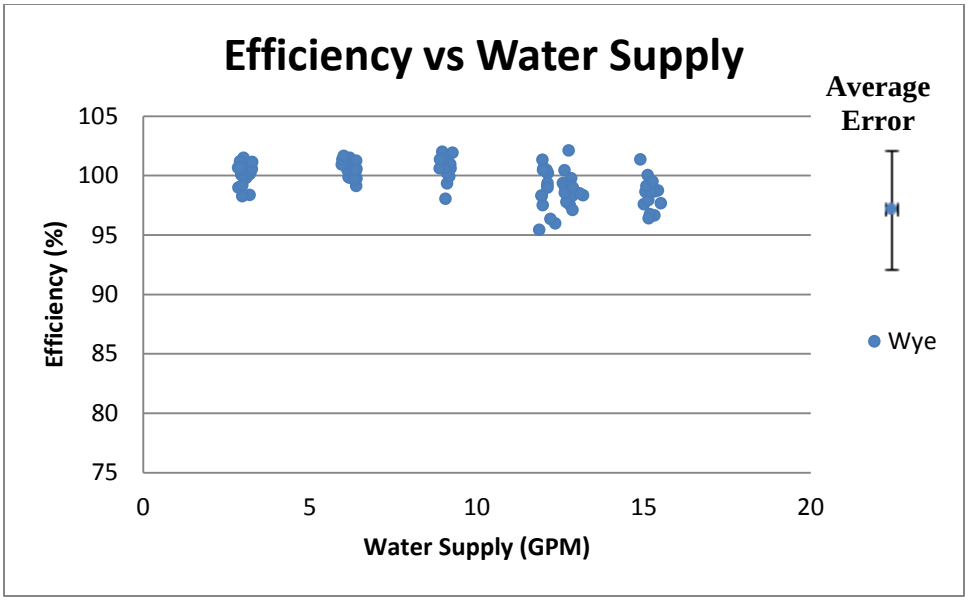

Figure 5.2. Comparison of the Water Supply and Efficiency for 4" Wye Fitting

Curiously, water flowrates below 10 GPM have a 2.5% to 4% range of values, while 12.4 GPM has a range of 6.73% and 15.2 GPM actually drops its range to 5%. This indicates that GVF, velocity, or pressure has an important impact on efficiency at higher flowrates. Also needing consideration is air entrainment, which occupies a substantial portion of the separator at higher water flowrates, discussed later in the results.

Table 5.3 shows the flowrates for the tee pipe fitting for the same 4” separator. As expected, the GVF, velocity, and water flowrate values are all very similar to the wye tests. However, the tee performed slightly better in efficiency than the wye.

Table 5.3. Water Flowrates for the 4" Tee Fitting

Average GVF	Average Velocity (m/s)	Average Water Flowrate (GPM)	Average Efficiency (%)	Standard Deviation (%)
0.990	2.50	2.94	100.71	0.42
0.953	0.54	3.07	99.50	0.58
0.950	1.00	6.02	101.48	0.58
0.900	0.50	6.39	100.37	0.44
0.951	1.53	9.10	99.84	1.56
0.951	2.03	12.16	99.45	1.00
0.903	1.03	12.76	99.47	1.52
0.950	2.52	15.22	98.57	1.60

Figure 5.3 shows the relationship between efficiency and water supply flowrate. Before 10 GPM, the fitting performs close its theoretical limit with an average efficiency of 100.4%, exactly the same 100.4% average of the wye fitting (although smaller with rounding error). At 12.5 GPM, the drops to 99.5% and at 15.2 GPM, the efficiency reaches 98.6%.

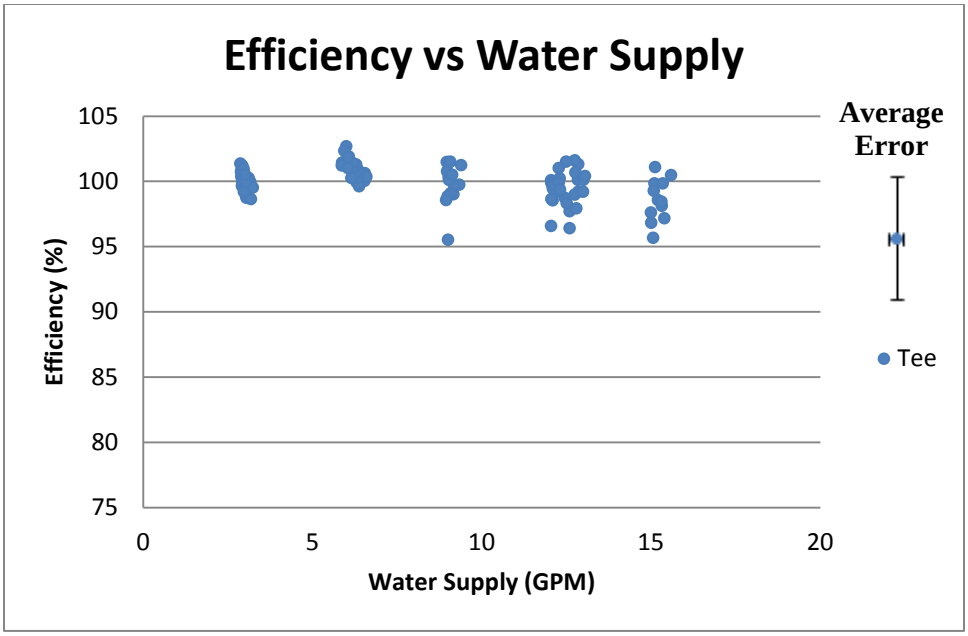

Figure 5.3. Comparison of the Water Supply and Efficiency for 4" Tee Fitting

Similar to the wye pipe fitting, the deviation seems to increase with increase flowrate, suggesting again that pressure, velocity, GVF, or the level of air entrainment has significant effects on efficiency at higher flowrates.

Figure 5.4 provides an overlay of the tee and wye pipe fitting results and they appear remarkably similar. In fact, if similar mixture conditions existed similar to the experimental setup, the recommended pipe fitting would be the tee due to its lower cost. However, flows coming out of the exhaust end of the pump will be a more homogenous mixture, which the wye provides a theoretical advantage.

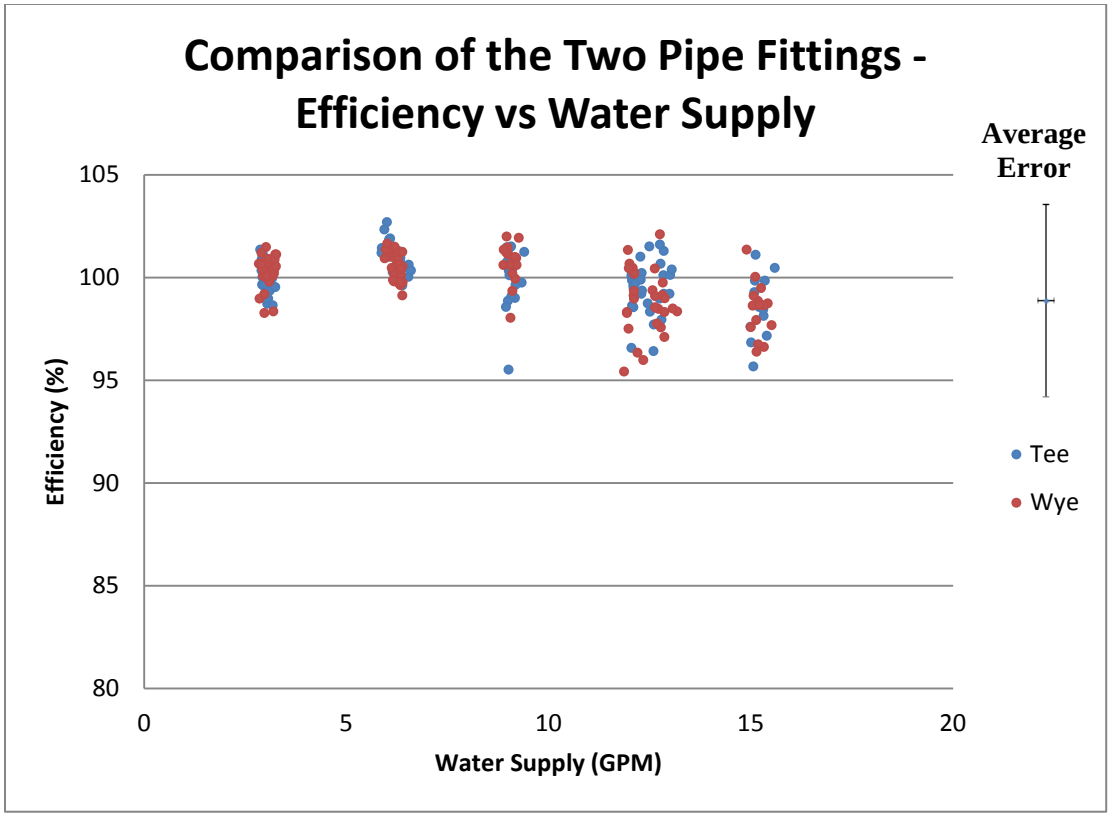

Figure 5.4. Comparison of the 4" Tee and Wye, Water Flowrate versus Efficiency

Table 5.4 shows the water flowrates and its corresponding efficiencies for the 6" separator. To reach the same GVF, velocity, and pressure the flowrates of both the air and water need to be increased. This allows testing for water flowrates beyond what the 4" separator can handle.

Table 5.4. Water Flowrates for the 6" Wye Fitting

Average GVF	Average Velocity (m/s)	Average Water Flowrate (GPM)	Average Efficiency (%)	Standard Deviation (%)
0.990	2.56	6.48	100.61	1.06
0.951	0.51	6.80	100.61	0.39
0.950	1.00	13.47	100.40	0.54
0.901	0.51	14.31	99.84	0.39
0.949	1.50	20.60	99.09	1.19
0.951	2.06	27.06	97.22	2.37
0.900	0.98	28.06	98.04	1.96

Figure 5.5 shows the relationship between the water supply flowrate and efficiency. The 6” separator has the same initial efficiency as the 4” separator. Flowrates below 15 GPM have an average efficiency of 100.4%. At 20.6 GPM, the efficiency drops to 99.1% and at 27.6 GPM, the efficiency finally falls to 97.6%.

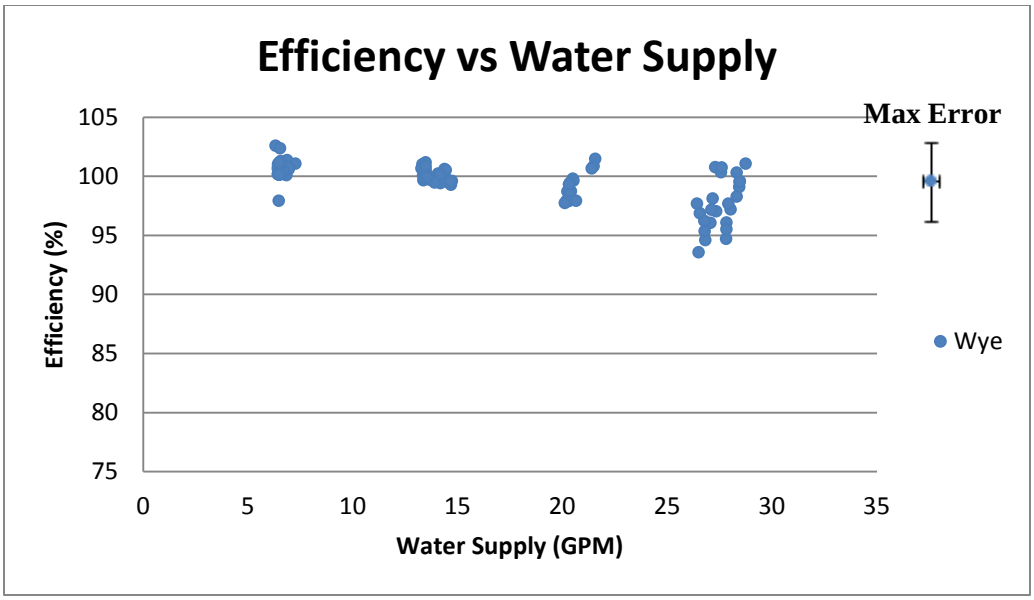

Figure 5.5. Comparison of Water Flowrate and Efficiency for the 6" Wye Fitting

The 6” has a more defined drop in efficiency at the same air velocities than the 4” separator. In addition, the standard deviation is also higher, and again appears to rise with increasing water flowrates. This may suggest some parameters may act independently or do not scale linearly with an increase in cross sectional area.

Figure 5.6 compares water supply flowrate and efficiency for all pipe fittings. The 6” separator’s better effectiveness at higher flowrates is especially prevalent at water flowrates between 10 and 15 GPM. The 4” separator’s efficiency starts to decline while the 6” separator is near 100% efficient.

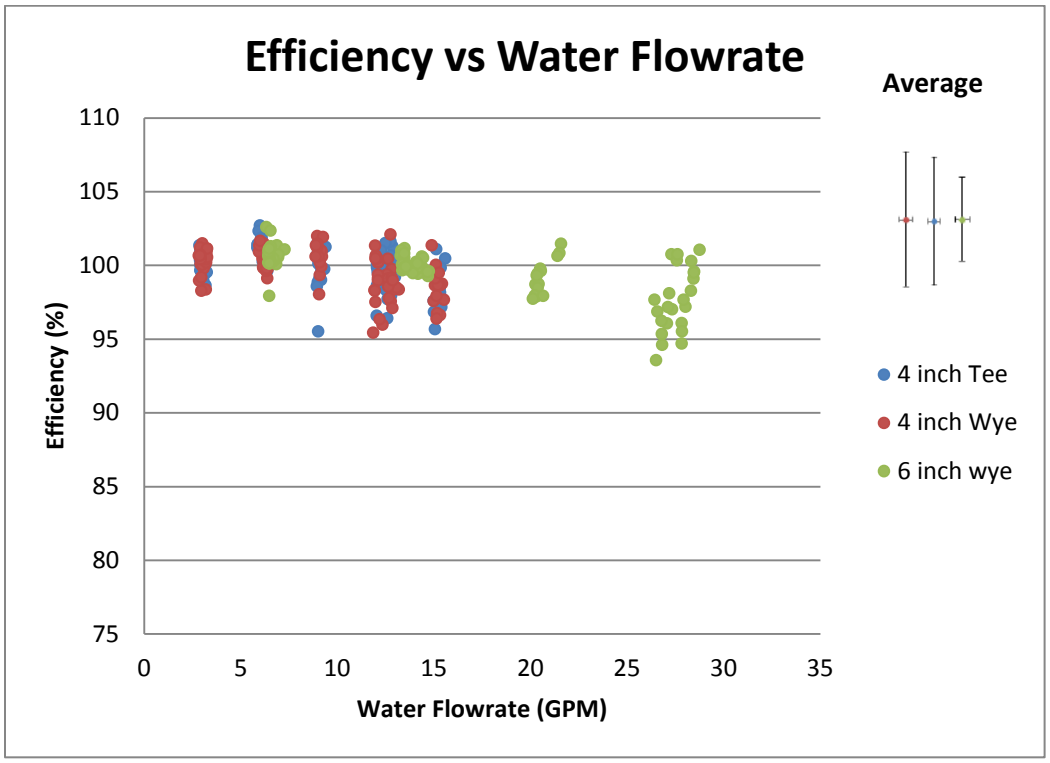

Figure 5.6. Comparison of Water Flowrate and Efficiency for all Fittings

These results lead to the first design parameter(5.2). Multiplying the air velocity and GVF gives a constant that provides 100% efficiency. This equation assumes no liquid carryover, and exceeding 0.075 results in potential losses in efficiency

$$v_g * (1 - GVF) = 0.075 \tag{5.2}$$

5.1.2. Pressure

Pressure is significant due to its potential to span a significant variation of values. Pressures used in this experiment include 15, 30, 45, 60, and 75 psi. However, at the exhaust end of a pump, the pressure could be as large as 1,500 psi [2]. Because of this large variance, the pressure is an important factor to study.

Air and other gasses have the natural ability to compress. Assuming 100% compressibility and a barometric pressure of 14.7 psi, a 15 psi to 60 psi or a 30 psi to 75 psi compression doubles the mass flowrate and momentum, at constant velocity conditions (the standard which will be used in this experiment). This results in higher forces preventing separation between water and air. At constant mass flowrate conditions, however, an increase in pressure represents a decrease in momentum from the resulting decrease in air velocity. At this condition, separation between water and air is more favorable.

At lower water flowrates there appears to be little variation in results; however, at higher flowrates, there is a significant variation in efficiencies. This suggests higher water flowrates is the area that most needs to be studied. Figure 5.7 shows the

relationship between pressure and efficiency for the 4” wye pipe fitting at 12.4 GPM water flowrate. At 90% GVF, there seems to be little to no effect from pressure on efficiency. At 95% GVF, there is a decrease in efficiency after 45 psi. This difference may be due to the fact the 90% GVF flow exists at 1.0 m/s and the 95% GVF exists at 2.0 m/s, suggesting that pressure variance is important at larger velocities.

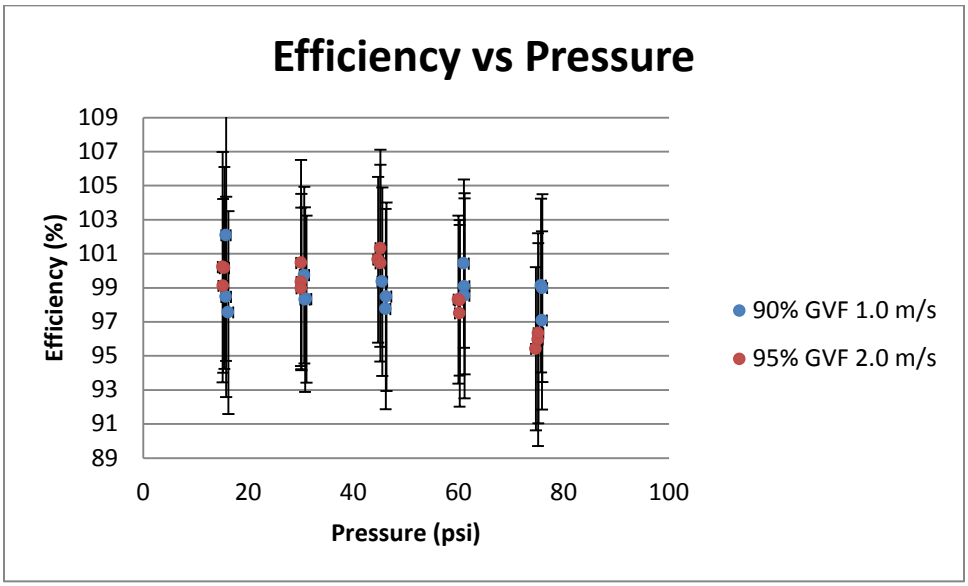

Figure 5.7. Comparison of Pressure and Efficiency for the 4" Wye Fitting

Figure 5.8 compares the pressure and efficiency at 95% GVF for the 6” separator. Similar to the 4” results, the pressure has little to no effect on efficiency at lower velocities. At higher velocities, the effect pressure has on efficiency is more and more prevalent. 2.0 m/s shows the maximum changes, while each subsequent velocity has

smaller and smaller changes. This is a strong indicator that the pressure's effect on efficiency is highly dependent on the velocity of the system.

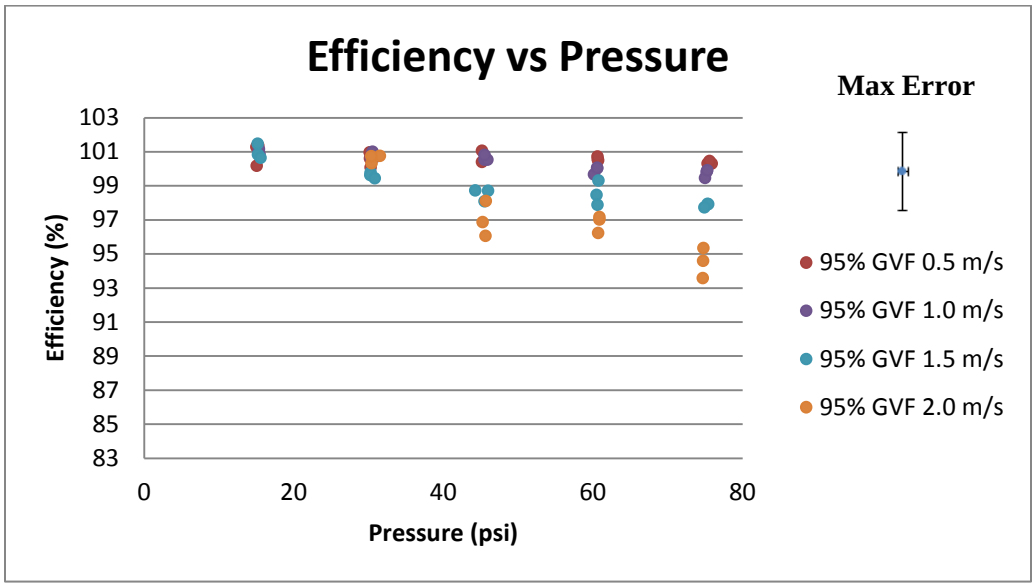

Figure 5.8. Comparison of Pressure and Efficiency for the 6" Wye Fitting

5.1.3. Velocity

Velocity plays in important role in drag force, as evidence by equations (3.12) and (3.17). Velocity is easily manipulated by changing the area of the separator if the mass flow rate of air and water is held constant. At any defined air velocity and separator diameter, the volumetric flowrate of air will be constant over varying GVF. By specifying pressure in addition to velocity and the diameter, the mass and volumetric flowrates of air will be constant at specific GVFs.

Figure 5.9 shows the relationship between velocity and efficiency for the 4” tee pipe fitting. At 1 m/s and 2.5 m/s there is a decrease in efficiency with a decrease in GVF. This phenomenon is the result of an increase of water flowrate with the decrease in GVF, as describe in Section 5.1.1. There does seem to be a negative trend with increasing velocity, especially when comparing constant GVFs. However, there is no clear indication whether the velocity affects efficiency independently of water flowrate. At 99% GVF at 2.5 m/s the results display higher efficiencies than 90% and 95% GVFs at 0.5 m/s, which enhances the ambiguity.

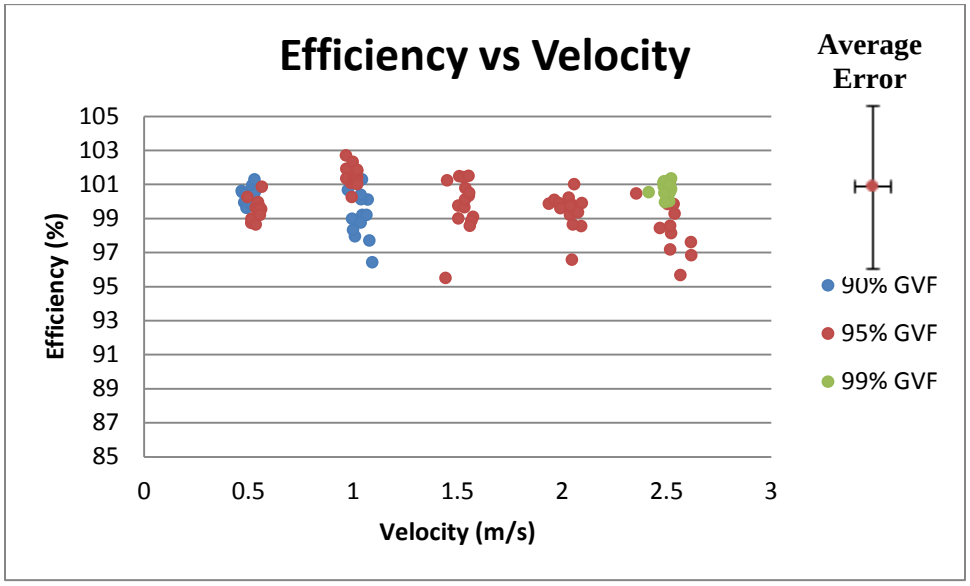

Figure 5.9. Comparison of Efficiency and Velocity for 4" Tee Fitting

Figure 5.10 shows the relationship between velocity and efficiency for the 6” separator. Again, the relationship between water flowrate and efficiency is clear, but

between velocity and efficiency, the relationship is not. The 99% GVF at 2.5 m/s does not reveal a decrease in efficiency when comparing 95% and 90% GVF at 0.5 m/s. The trends do not show any loss in efficiency that cannot be described by the water flowrate and pressure.

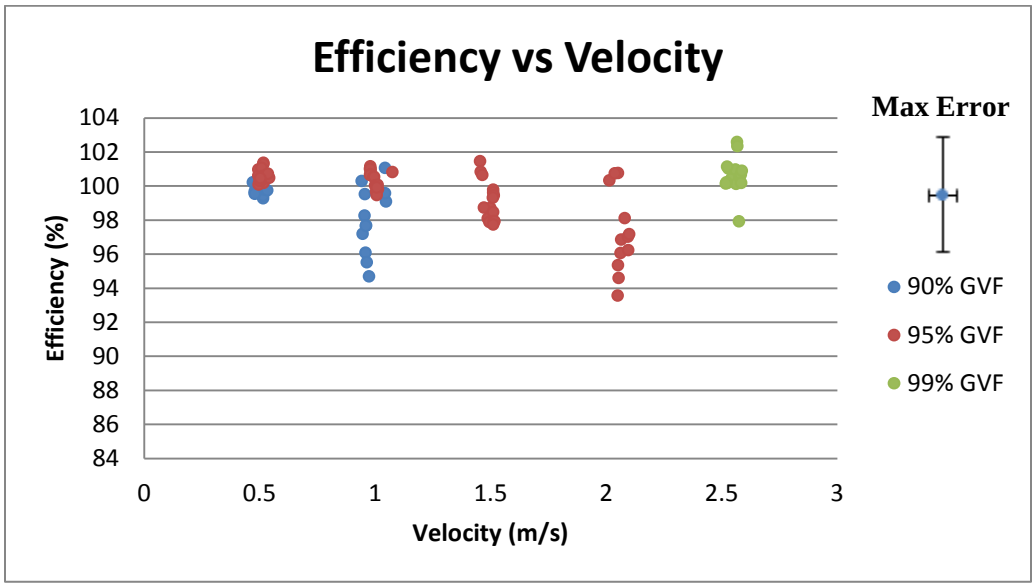

Figure 5.10. Comparison of Velocity and Efficiency for the 6" Wye Fitting

Even though the results are inconclusive on whether velocity has an impact on efficiency independently of pressure and water flowrate, there are some ideas which are still clear. By increasing from 4” to 6”, there is a decrease in velocity with an increase in efficiency with constant mass flowrates of air and water. This provides evidence that pressure effects on efficiency are dependent on velocity, but does not give the same

conclusions to water flowrate. The increase in efficiency for higher flowrates can be explained from the higher volume.

Velocity and its effect on droplet size could be a continued area of study. The experiment's ability to create a homogenous mixture is inadequate to measure this effect. This could provide data which could determine whether the wye is a better choice as the pipe fitting than the tee. However, air entrainment could render this concern moot, as the residence time could be too low to allow high enough velocities while maintaining a constant GVF.

5.2. Air Entrainment Study

Air entrainment in the standing level of water inside the separator is as important variable as pressure and velocity, but there is a need to separate it because of its reliance on visual data instead of measured data. At higher water flowrates, there is significant variance which is not explained solely by analyzing pressure and velocity. Analyzing the length of air entrainment (L_{AE}) can provide answers on to how design a better separator.

The problems air entrainment cause in the separator is twofold. First, air entrainment creates disturbances in the pipe fitting that has the potential to force water or other liquids upward. Having the air entrainment too close to the fitting has the potential to reduce efficiency.

Second, if air becomes trapped in the water exiting the bottom of the separator, the flowmeter will read higher water flowrates than what is actually going through the flowmeter. In order to rectify this problem, the liquid level must be high enough from the liquid exit so the entrained air can escape from the water while still inside the separator.

Both problems indicate the correct water level is the one which does not allow the air entrainment to interfere with the pipe fitting or the water exit. The air entrainment is studied using a video camera to observe how L_{AE} varies with GVF, velocity, pressure, and separator diameter.

Figure 5.11. Example of Air Entrainment

Figure 5.11 gives an example of air entrainment in the separator. The top, clear area is where the water drops to the standing water level. The white, frothy area is where the air entrainment exists. The dark area underneath everything is where water exists free from air. The measuring tape to the left of the separator is used as a scale to determine L_{AE}. The actual water height is approximately half way between the top and bottom of the frothy mixture. The water height is defined as the level of standing water if air entrainment was completely removed. The differential pressure transducer measures this value and does not measure the height of the liquid column plus all air trapped in the

water. The LED light is on, indicating the LabVIEW program is collecting data. Figure 5.12 shows the analysis used to determine air entrainment level.

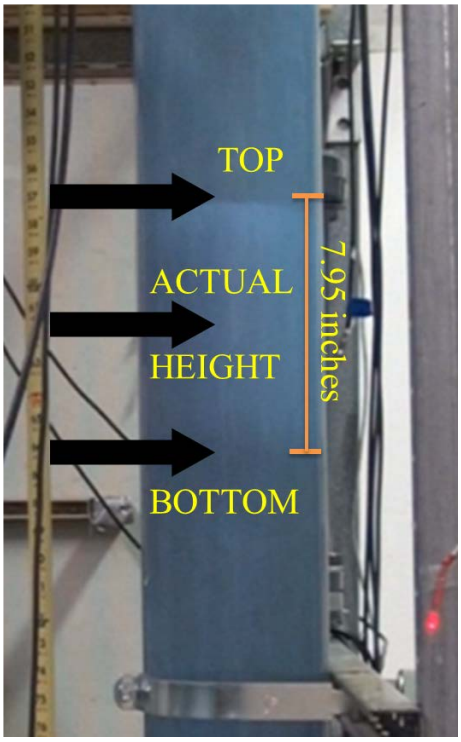

Figure 5.12. Air Entrainment Detailed

Tests were run for all three pipes fittings at GVFs of 90%, 95%, and 99% at a velocity of 1.0 m/s and a pressure of 60 psi. Data was taken for pressures of 30, 45, 60, and 75 psi at 95% GVF and a velocity of 1.5 m/s. Lastly, included in the results are velocities of 1.0, 1.5, and 2.0 m/s at 95% GVF and a pressure of 60 psi. The results are included in Table 5.5. Included in the results is τ', which is defined in 5.2.2.

Table 5.5. Air Entrainment Results

Fitting	D_s (in)	Pressure (psi)	GVF (%)	Velocity (m/s)	Water Flowrate (GPM)	L_{AE} (in)	τ' (s/in)
wye	3.768	60.0	0.950	1.01	6.08	3.15	0.476
		60.1	0.902	1.03	12.84	30.41	0.226
		60.0	0.992	1.02	1.75	0.49	1.654
		29.9	0.950	1.53	9.28	6.10	0.312
		44.9	0.950	1.47	8.99	5.84	0.322
		60.0	0.950	1.50	9.19	6.76	0.315
		74.9	0.951	1.52	8.99	5.95	0.322
		59.8	0.948	1.96	12.51	40.87	0.232
tee		61.3	0.985	0.99	2.01	2.12	1.444
		60.0	0.951	1.01	6.03	3.03	0.480
		59.9	0.900	1.00	12.72	70.57	0.228
		30.0	0.950	1.46	8.83	4.36	0.328
		44.9	0.951	1.53	9.14	7.92	0.317
		60.1	0.950	1.54	9.25	8.83	0.313
		75.8	0.951	1.55	9.07	33.21	0.319
		60.0	0.947	1.96	12.59	44.14	0.230
wye	5.660	60.0	0.990	1.01	2.63	0.66	2.487
		60.1	0.949	1.00	13.74	5.48	0.476
		60.5	0.900	0.99	28.36	65.97	0.230
		30.0	0.949	1.46	20.09	10.14	0.325
		45.1	0.949	1.50	20.66	16.33	0.316
		59.9	0.951	1.50	20.00	14.74	0.327
		75.2	0.951	1.51	19.94	20.44	0.328
		60.1	0.950	2.00	26.93	76.38	0.243

5.2.1. Water Flowrate

Similar to efficiency, water flowrate has the highest impact on L_{AE}. Figure 5.13 shows how the water flowrate affects L_{AE}. Curiously, the results follow an exponential path with only small deviations. This means when designing a separator, the length of

the pipe used as the water collection leg has to be exponentially longer for higher flowrates to allow liquid exiting the bottom of the separator to be free from gas.

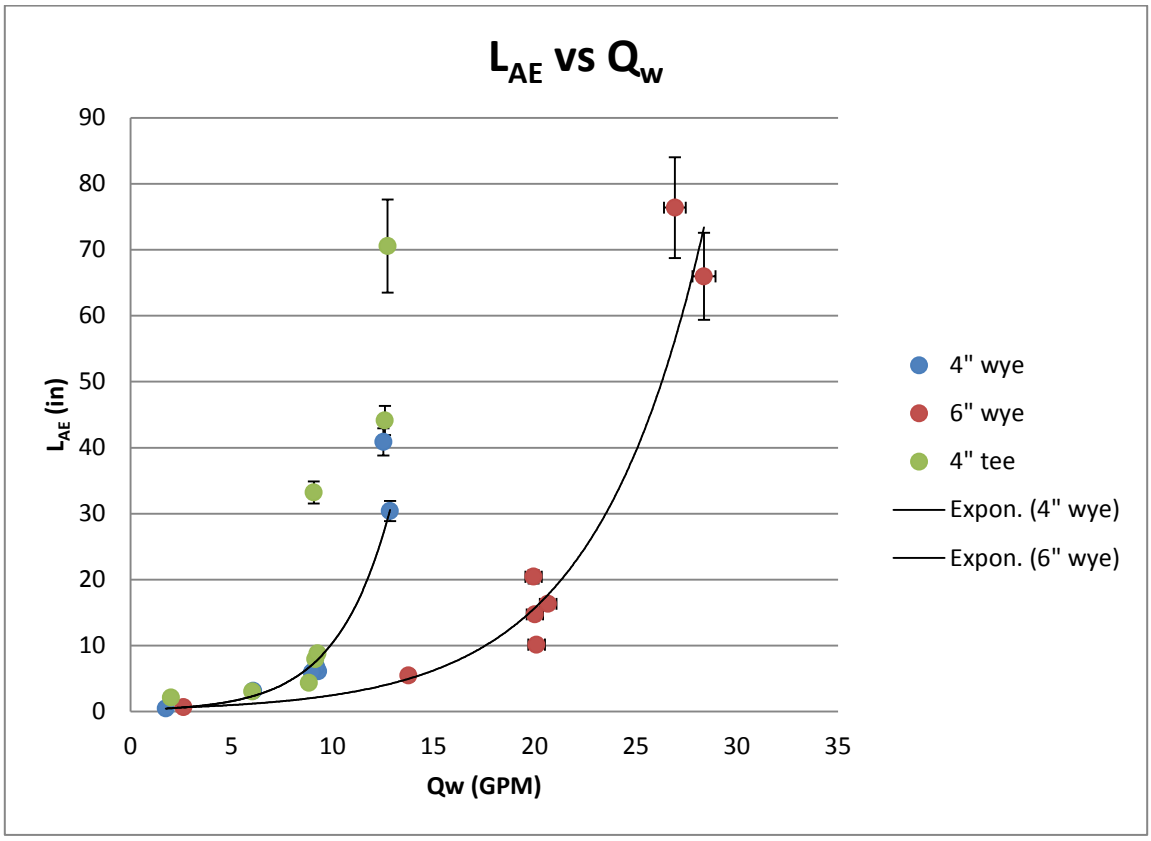

Figure 5.13. Comparison of L_{AE} and Water Flowrate

Figure 5.14 removes variations due to velocity and pressure and compares the effects of GVF (which is directly related to water flowrate) to the L_{AE} at a pressure of 60 psi and a velocity of 1.0 m/s. The wye results show near perfect examples of exponential data, although the number of data points is low. The tee, however, is close to the 4 inch wye

results at 95% and 99% GVF, but deviates by a large margin at 90%. This is something that will be discussed in section 5.2.5.

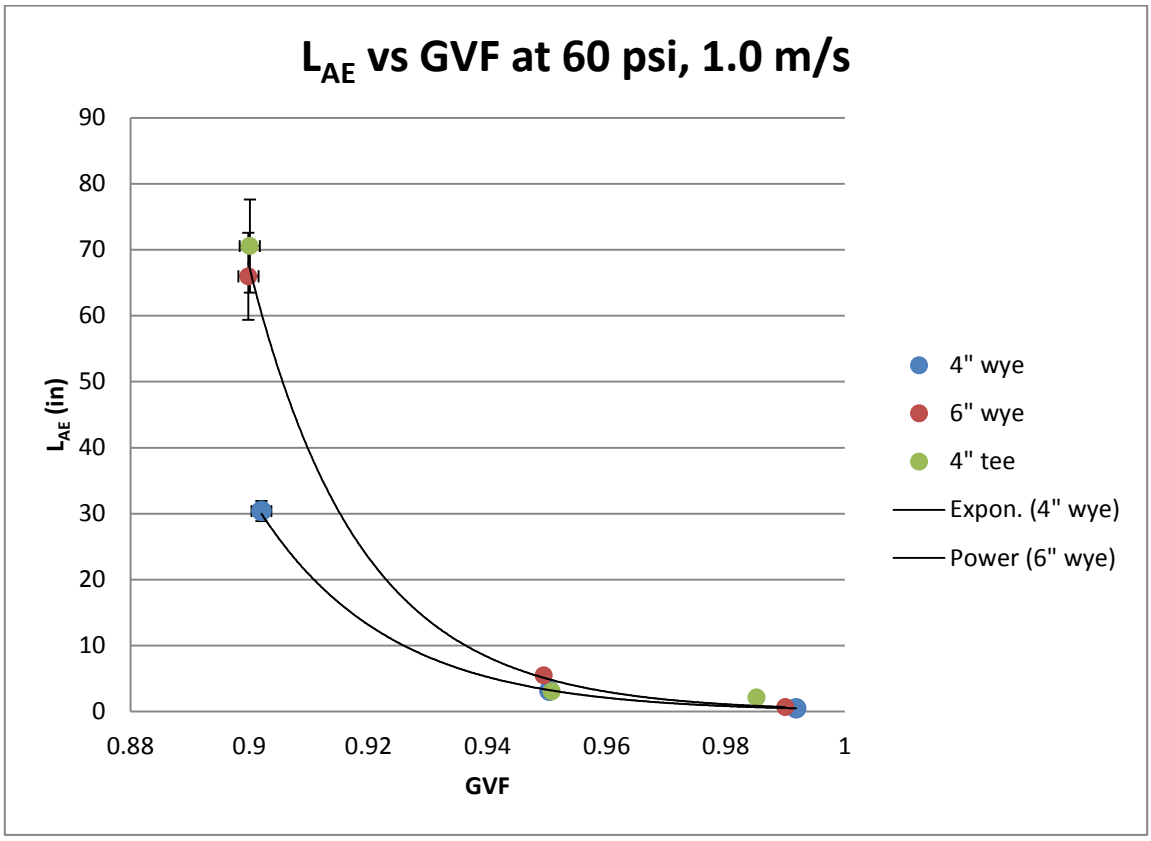

Figure 5.14. Comparison of GVF and L_{AE}

5.2.2. Residence Time

Residence time is a significant variable for all separators. The low residence time compared to conventional gravity separators emphasizes its importance. Due to the residence time being dependent on the height of the column of water and the difficulty to hold the level constant throughout all tests, a new parameter is devised, τ', which is the

residence time per the height of the water column, devised in equation(5.3). Q_w represent the water flowrate which exits through the bottom of the separator and not the water flowrate entering the separator in the air-water mixture.

$$\tau' = \frac{\tau}{h} = \frac{\pi * D_s^2}{4 * Q_w} \tag{5.3}$$

Due to the consistency of the results, an equation is proposed to equate L_{AE} to τ' and D_s(5.4). This is the second design equation used to determine the appropriate separator design. All units are expressed in terms of seconds or inches.

$$L_{AE} = 0.0135 * D_s^2 * e^{\frac{1.156}{\tau'}} \tag{5.4}$$

Figure 5.15 compares equation (5.4) to the results found on Table 5.5. The results show that there is an ideal minimum value τ' at 0.5 s/in for an efficient measurement of the required height of pipe for the bottom portion of the separator. Values below 0.5 s/in exponentially increase L_{AE}, requiring larger separator lengths. If the separator length is not the largest constraint for operation, τ' can be decreased for a higher extraction of water or lower pipe diameters.

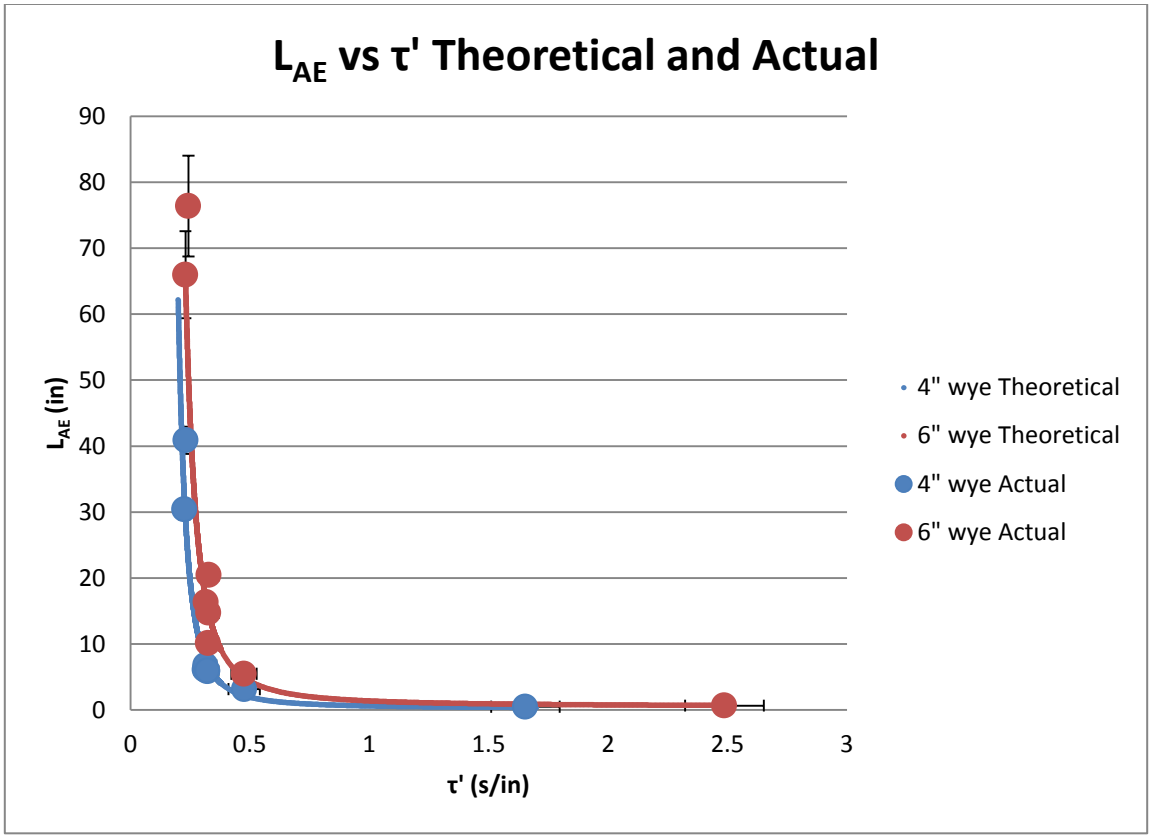

Figure 5.15. Comparison of Theoretical and Actual τ' and L_{AE}

The relationship between Q_w and τ' is defined in Figure 5.16. By specifying the flowrate required by the seal flush, the ideal diameter can be determined using the τ' of 0.5 s/in. If the diameter and water flowrate is fixed, the τ' can be found and used in equation(5.4) to find the corresponding L_{AE}.

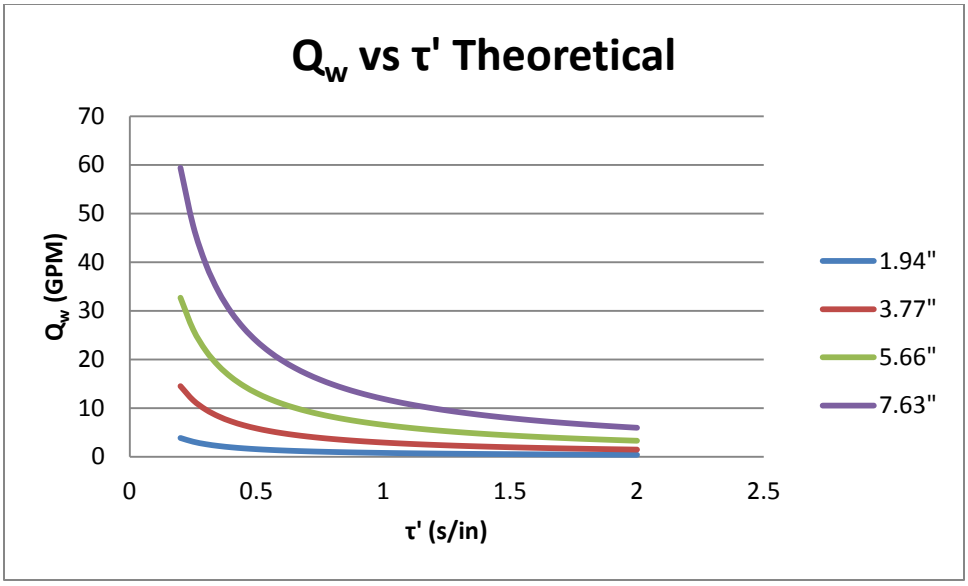

Figure 5.16. Comparison of Q_w and τ' for Schedule 80 PVC Diameters

5.2.3. Pressure

The effect of pressure is difficult to understand. Figure 5.17 shows the relationship between pressure and L_{AE} at 1.5 m/s and 95% GVF. The results are overall ambiguous. The 4" wye shows almost no effect whatsoever. The 4" tee follows a similar path before providing another erroneous result at 75 psi. The 6" wye shows an increasing trend, but is inconsistent. It is important to note that L_{AE} actually doubles from 30 psi to 75 psi in the 6" separator.

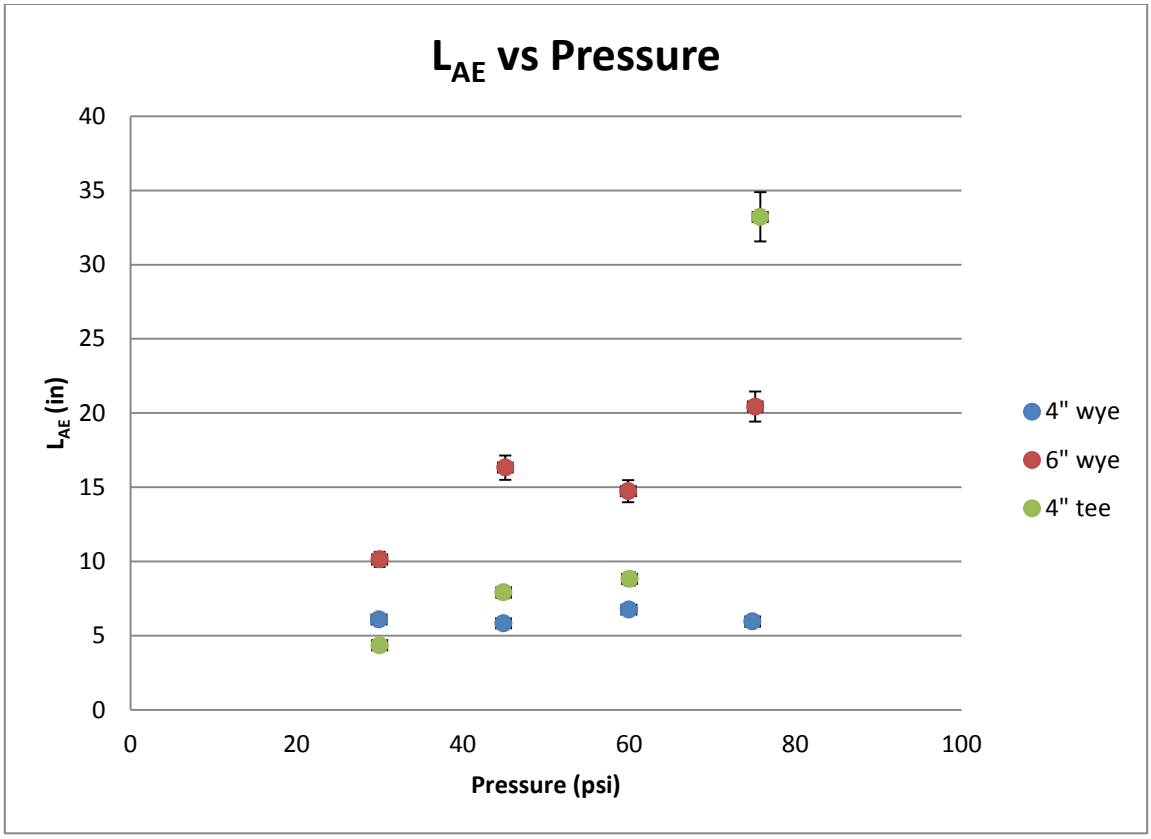

Figure 5.17. Comparison of Pressure and L_{AE}

5.2.4. Velocity

Velocity is another difficult parameter. Due to its relationship with water flowrate, it is problematic to uncover valuable insight on its effects. Figure 5.18 shows the relationship between velocity and L_{AE} using a pressure of 60 psi and a GVF of 95%. For the first time, the tee pipe fitting provided results without excessive amounts of air entrainment. The results are nearly identical to the 4" wye. Curiously, the 6" results are approximately 92% higher than the 4" result at every velocity.

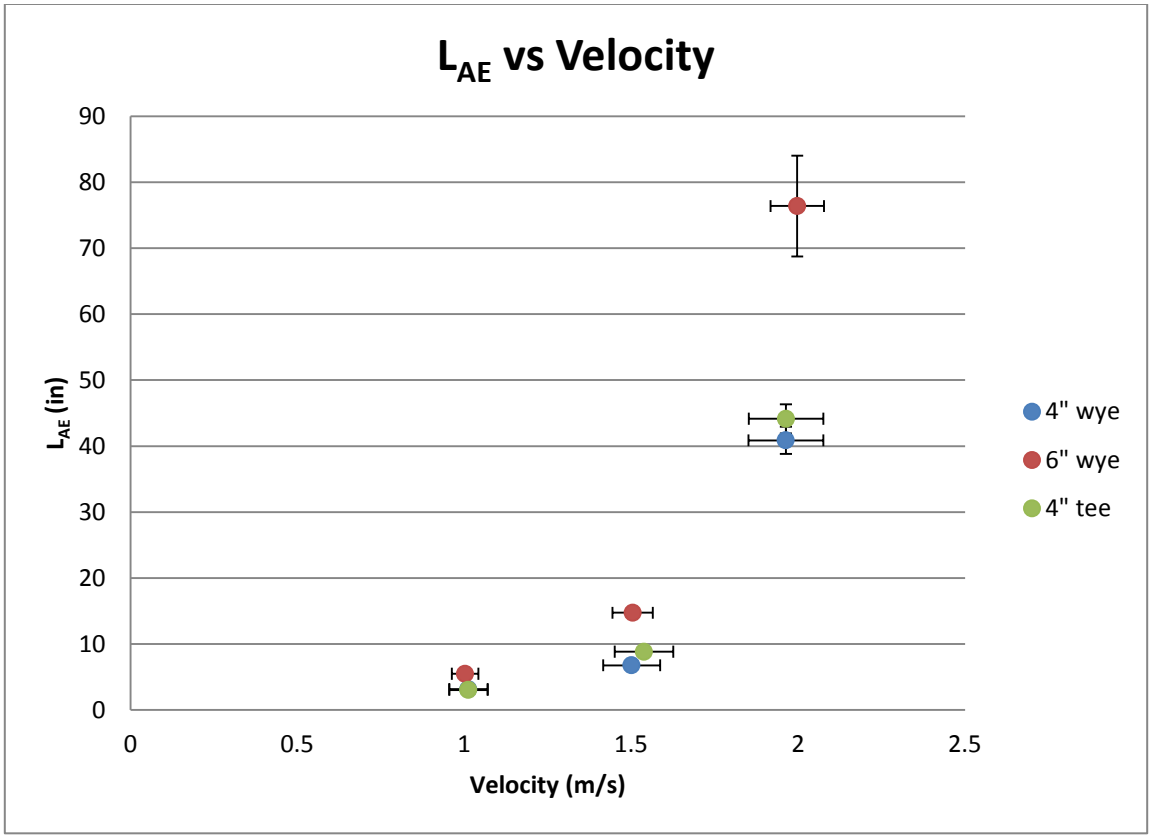

Figure 5.18. Comparison of Velocity and L_{AE}

5.2.5. Tee versus Wye

The tee and wye are nearly identical for almost the results, except for two data points. This leads to two possible conclusions. Either the results are erroneous and are not indicative of the true tee performance or the tee design allows for abnormal high L_{AE} if the correct conditions are met. Figure 5.19 shows the air entrainment in the 4" separator for the wye pipe fitting 90% GVF, 1.0 m/s, and 60 psi. Figure 5.20 shows the air entrainment for the tee pipe fitting at the same conditions.

Figure 5.19. Air Entrainment in the Wye Pipe Fitting

Figure 5.20. Air Entrainment in the Tee Pipe Fitting

As the data shows, the LAE in the tee is much larger than in the wye. It even appears that the bubbles are larger in the tee. The larger air bubbles are from an unknown cause. This leads to speculation that the tee fitting has a design flaw which is not present in the wye. Ultimately, this single flaw suggests that the wye is a better component to separate flow.

6. CONCLUSION

The objective of this study was to determine if a simple separator design could be used to extract liquid from the exhaust of a multiphase pump to the meet the seal flush requirements while maintaining minimal gas capture at high GVF conditions. Two pipe fittings, a tee and a wye, are used and along two schedule 80 PVC pipes, 4" and 6", to determine the potential usage of a minimal separator design. The first investigation looked at the separator's efficiency at varying GVFs, velocities, pressures, and diameters. The second investigates focuses on L_{AE} and how it related to varying GVFs, velocities, pressures, and residence times.

Section 6.1 recapitulates the efficiency results. The 4" and 6" designs are compared to display how increases in area allow for higher removal of water. Section 6.2 describes the results from air entrainment. A new variable is introduced, τ', as a design parameter. Section 6.3 defines the design parameters for a separator specific to the needs and constraints of the operation. Section 6.4 gives recommendations on future research.

6.1. Efficiency Performance

The experimental results provide detailed efficiency curves. Water flowrate provides the most effect on efficiency. The tee and wye pipe fittings possess extremely similar efficiency curves. Efficiency is 100% up until 10 GPM in the 4" pipe, then dips, but not

at a consistent rate. The 6” separator provides higher water flowrate handling capabilities. The 6” separator can handle flowrates up to 15 GPM before seeing a dip in efficiency. The inconsistencies of results at higher flowrates suggest pressure, velocity, and L_{AE} can have significant effects on efficiency at higher flowrates.

Pressure provides inconsistent results. For the 4” separator, at lower velocities (1 m/s) the pressure has little effect on efficiency. At higher velocities (2 m/s) effect is minimal, but there does exist a negative trend. For the 6” separator, pressure effects are more obvious and seem to increase with increasing velocities. This leads to the conclusion that pressure effects on efficiency are only important at higher velocities.

As velocity increases, the efficiency decreases, in general. At lower flowrates, such as below 10 GPM for the 4” separator and 15 GPM for 6” separator, velocity has no effect on efficiency. After those flowrates, efficiency curves show definitive reductions with increasing flowrates. As previously mentioned, pressure works in tandem with velocity, suggesting that keeping the velocity below 1.5 m/s at 95% GVF or 0.75 m/s at 90% GVF (hinting that this is also true at 7.5 m/s for 99% GVF) is an optimal strategy for reducing effects of velocity and pressure on efficiency.

6.2. Air Entrainment Performance

The air entrainment investigates required the use of transparent pipe and a video camera to record the results. Air entrainment exists in the separator as a white, frothy

mixture that is easily identifiable with a video camera. The measured height of the liquid column used to determine residence time and efficiency is half way between the top and bottom of the air entrainment. Using this knowledge, L_{AE} can be compared against the water flowrate, GVF, velocity, diameter, and τ'.

Water flowrates affects L_{AE} at an exponential rate. Converting the water flowrate to τ', an equation is derived that relates τ', D_s, and L_{AE}. This equation is used to produce specifications that fit the needs set forth by the pump. This equation works due to the 45% difference between the 4" and 6" curves, which is the same as value as the ratio of the 4" and 6" areas.

Pressure provides more ambiguous results. The 4" separator for both the tee and wye shows little to no changes in L_{AE} from pressures between 30 and 75 psi. The 6" separator shows increases in L_{AE}, but at an inconsistent rate. The results are at a velocity of 1.5 m/s, so there is no indication whether changes in L_{AE} increases with varying pressures at higher velocities.

Changes in velocity are closely tied to water flowrate and are exponentially coupled with L_{AE}. The 4" wye and tee pipe fittings provide nearly identical results at 95% GVF and 60 psi. The 6" separator has a consistent increase of 92% over the 4" results, again suggesting L_{AE} can be modeled mathematically.

6.3. Design Parameters

This study sets forth two equations which aids in the design the meet seal criteria and flow characteristics along with the possibility of two pipe fittings to use in separation. Equation(5.2) multiplies the gas velocity and gas volume fraction. Equation(5.4) defines L_{AE} as a function of D_s and τ'.

By keeping v_g*(1-GVF) below 0.075, the separator can achieve 100% efficiency. This equation makes two assumptions. First, there is enough separator length to achieve proper results. Also, increasing the separator length beyond what is necessary does not show to improve the results set forth by the equation. Second, 100% of the water brought in through the mixture is intended to be separated.

Keeping τ' above 0.5 s/in is useful to creating a compact separator design. Reducing τ' causes the minimum length of pipe needed to separate the water and air exponentially increase. By defining the required flowrate and using a τ' of 0.5 s/in, the D_s and L_{AE} can be found.

The tee and wye pipe fittings provide nearly identical results over most of the experimental tests. Normal, this would suggest that the cheaper option, the tee, would be the recommended fitting. However, two air entrainment tests suggest that a design flaw in the tee allows for unusually high L_{AE} if the right conditions are met. This design

flaw is not seen in the wye, signifying that the wye is the ideal pipe fitting to use in this separator design.

6.4. Recommendations for Future Work

In order to better understand the effectiveness of the separator, more research needs to be performed.

- The lack of a homogenous mixture reduces the ability to determine if velocity has an impact on efficiency at lower water flowrates and whether the theoretical advantage of the wye is significant.
- Different fluids, such as natural gas and oil, and how the changes in viscosity and density change results
- Higher pressures to see if the increase in momentum has a significant impact on L_{AE} and efficiency.
- Why the tee suddenly creates high L_{AE}.
- More tests should be implemented to expand the τ' an L_{AE} equation to include varying velocities and pressures.

REFERENCES

[1] Stewart M, Arnold K. Gas-liquid and liquid-liquid separators. Elsevier; 2008.

[2] Smith HV. Oil and gas separators. In: Petroleum engineers handbook, Richardson, TX: H. B. Bradley, S.P.E; 1987, Chapter 12.

[3] Kouba GE, Shoham O, and Shirazi S, Design and performance of gas-liquid cylindrical cyclone separators. International Meeting on Multiphase Flow, Cannes, France; June 1995.

[4] Wang S, Gomez LE, Mohan RS, Shoham O. Gas-liquid cylindrical cyclone (GLCC) compact separators for wet gas applications. Engineering Technology Conference on Energy, Houston, Texas; February 2001.

[5] Chirinos WA, Gomez LE, Wang S, Mohan RS, Shoham O, et al. Liquid carry-over in gas/liquid cylindrical cyclone compact separators. SPE Journal, 2000;5(3):259-267.

[6] Mohan RS, Wang S, Shoham O, Kouba GE. Design and performance of passive control system for gas-liquid cylindrical cyclone separators. Journal of Energy Resources Technology, 1988;120:49-55.

[7] Laleh AP. CFD simulation of multiphase separators. Dissertation, University of Calgary; September 2010.

[8] Kabir CS, Hasan AR. Performance of a two-phase gas/liquid flow model in vertical wells. Journal of Petroleum Science and Engineering, 1990;4(3):273-289.

[9] Taitel Y, Barnea D, Dukler AE. Modeling flow pattern transition for steady upward gas-liquid flow in vertical tubes. AIChE Journal, 1980;46:345-354.

[10] Stewart AC, Chamberlain NP, Irshad M. A new approach to gas-liquid separation. SPE European Petroleum Conference, The Hague, The Netherlands; October 1998.

APPENDIX A – GAS VOLUME FRACTION CALCULATION

Inputs

P_a = 110.7 psi
P_m = 30.51 psi
Q_i = 1139 Hz
Q_{wi} = 307 Hz
T_a = 81.99 F
T_w = 87.15 F

Calculations

Air Density of The Air Inlet (ρ_{ai}) = (110.7+14.7)*6.894757 / (.287*(81.99+459.67)*5/9) = 10.011 kg/m3

Air Density of the Mixture Air (ρ_{am}) = (30.51+14.7)*6.894757 / (.287*(87.15+459.67) *5/9) = 3.575 kg/m3

Volumetric Flowrate of the Air Inlet (Q_{ai}) = (1139 – 2)*.016239 = 18.463 ACFM

Volumetric Flowrate of the Air Mixture (Q_{am}) = (18.463*10.011/3.575) = 51.702 ACFM

Volumetric Flowrate of the Water (Q_{wi}) = (307 – 2)*.067374 = 20.549 GPM

Outputs

GVF = 51.702/(20.549*.1337 + 51.702) = .9495

APPENDIX B – VELOCITY CALCULATION

Inputs

P_a = 110.7 psi
P_m = 30.51 psi
Q_i = 1139 Hz
T_a = 81.99 F
T_w = 87.15 F
D_s = 5.66033

Calculations

Air Density of The Air Inlet (ρ_{ai}) = (110.7+14.7)*6.894757 / (.287*(81.99+459.67)*5/9) = 10.011 kg/m3

Air Density of the Mixture Air (ρ_{am}) = (30.51+14.7)*6.894757 / (.287*(87.15+459.67) *5/9) = 3.575 kg/m3

Volumetric Flowrate of the Air Inlet (Q_{ai}) = (1139 – 2)*.016239 = 18.463 ACFM

Volumetric Flowrate of the Air Mixture (Q_{am}) = (18.463*10.011/3.575) = 51.702 ACFM

Outputs

Velocity = 4*51.702*.0004719/(3.14159*(5.66*.0254)^2) = 1.503 m/s

APPENDIX C – UNCERTAINTY ANALYSIS

Uncertainty is measurement of error found in a measurement or calculation. Error can be found either in the instrument specifications or through propagation of other instrument errors.

Uncertainty through error propagation follows a general formula. R is the result of the function dependent on variables a, b, c …, which are independent, primary measurements.

$$R = f(a, b, c, \dots)$$

The uncertainty of R, U_R, is found as

$$U_R = \sqrt{\left(\frac{\partial R}{\partial a} U_a\right)^2 + \left(\frac{\partial R}{\partial b} U_b\right)^2 + \left(\frac{\partial R}{\partial c} U_c\right)^2 + \cdots}$$

C.1 Inlet Flowrate

Flowrate is defined from a frequency output and two calibration values

$$Q = (f + a) * b$$

This results in the equation

$$U_Q = b * U_f$$

U_f varies for different flowmeters. The air flowmeters show approximately 1% error, meaning U_f = .01*f. The low water flowmeter shows about 3% error and the medium flowmeter shows about 2%.

C.2 Pressure

Pressure uncertainty is 0.9 psi for the mixture and outlet values and 0.6 psi for the air inlet value.

C.3 Air Mixture Flowrate

The mixture flowrate can be expressed in the equation

$$Q_{am} = \frac{(P_i + 14.7) * T_m}{(P_m + 14.7) * T_i} * Q_{ai}$$

The uncertainty can be expressed as

$$U_{Q_{am}} = \sqrt{a^2 + b^2 + c^2 + d^2 + c^2}$$

$$a = \frac{(P_i + 14.7) * T_m}{(P_m + 14.7) * T_i} * U_{Q_{ai}}$$

$$b = \frac{U_{P_i} * T_m}{(P_m + 14.7) * T_i} * Q_{ai}$$

$$c = \frac{(P_i + 14.7) * T_m}{(P_m + 14.7)^2 * T_i} * U_{P_m} * Q_{ai}$$

$$d = \frac{(P_i + 14.7)}{(P_m + 14.7) * T_i} * Q_{ai} * U_{T_m}$$

$$e = \frac{(P_i + 14.7) * T_m}{(P_m + 14.7) * T_i^2} * Q_{ai} * U_{T_i}$$

U_{Qam} = 3.17%

C.4 GVF

GVF follows the equation

$$GVF = \frac{Q_{am}}{Q_{wi} + Q_{am}}$$

The uncertainty is expressed as

$$U_{GVF} = \sqrt{\left(\frac{Q_{am}}{(Q_{wi} + Q_{am})^2} * U_{Q_{wi}}\right)^2 + \left(\frac{Q_{wi}}{(Q_{wi} + Q_{am})^2} * U_{Q_{am}}\right)^2}$$

U_{GVF} = 0.37%

C.5 Velocity

Velocity follows the equation

$$v = \frac{4Q_{am}}{\pi D_s^2}$$

The uncertainty is expressed as

$$U_v = \sqrt{\left(\frac{4}{\pi D_s^2} * U_{Q_{am}}\right)^2 + \left(\frac{8Q_{am}}{\pi D_s^3} * U_{D_s}\right)^2}$$

U_v = 4.75%

C.6 dh/dt

dh/dt follows the equation

$$\frac{dh}{dt} = \frac{h_2 - h_1}{t_2 - t_1}$$

The uncertainty is expressed as

$$U_{\frac{dh}{dt}} = \sqrt{2 * \left(\frac{dh}{t_2 - t_1}\right)^2 + 2 * \left(\frac{(h_2 - h_1) * dt}{(t_2 - t_1)^2}\right)^2}$$

$U_{dh/dt}$ = 2.09%

C.7 Efficiency

Efficiency follows the equation

$$\eta = \frac{\pi D_s^2 \frac{dh}{dt}}{4Q_i}$$

The uncertainty is expressed as

$$U_\eta = \sqrt{\left(\frac{\pi D_s^2 U_{\frac{dh}{dt}}}{4Q_i}\right)^2 + \left(\frac{\pi D_s \frac{dh}{dt} U_{D_s}}{2Q_i}\right)^2 + \left(\frac{\pi D_s^2 \frac{dh}{dt} U_{Q_i}}{4Q_i^2}\right)^2}$$

U_η = 2.92%

C.8 Air Entrainment

The uncertainty in measuring LAE is considered 5% of the measured value due to the variations seen. However, when the LAE is measured using the actual liquid height from the differential pressure transducer, the uncertainty is considered 10% of the measured value.

C.9 τ’

τ’ follows the equation

$$\tau' = \frac{\pi D_s^2}{4Q_w}$$

The uncertainty is expressed as

$$U_{\tau'} = \sqrt{\left(\frac{\pi D_s U_{D_s}}{2Q_w}\right)^2 + \left(\frac{\pi D_s^2 U_{Q_w}}{4Q_w^2}\right)^2}$$

τ' = 13.9%

APPENDIX D – TABULATED RESULTS

Table D.1. 4" Wye Results

Pressure (psi)	dP	GVF	dGVF	Velocity (m/s)	dv	dV/dt (GPM)	d(dV/dt)	Qi (GPM)	dQi	η (%)	dη
15.26	0.9	0.8950	0.0041	0.466	0.064	6.26	0.23	6.26	0.19	99.9	4.8
15.16	0.9	0.8944	0.0042	0.464	0.064	6.27	0.23	6.29	0.19	99.7	4.7
15.26	0.9	0.8952	0.0041	0.466	0.064	6.33	0.22	6.25	0.19	101.3	4.7
30.60	0.9	0.8971	0.0035	0.481	0.039	6.34	0.25	6.34	0.19	100.0	4.9
30.69	0.9	0.8975	0.0035	0.482	0.039	6.35	0.26	6.31	0.19	100.6	5.1
30.08	0.9	0.8961	0.0035	0.481	0.039	6.33	0.26	6.39	0.19	99.1	5.1
45.36	0.9	0.9032	0.0031	0.503	0.034	6.18	0.26	6.19	0.19	99.8	5.1
45.27	0.9	0.9024	0.0031	0.497	0.033	6.19	0.28	6.18	0.19	100.2	5.4
45.44	0.9	0.9038	0.0031	0.505	0.034	6.16	0.23	6.16	0.19	99.9	4.8
60.70	0.9	0.8917	0.0033	0.460	0.028	6.38	0.23	6.40	0.19	99.7	4.7
60.38	0.9	0.9056	0.0029	0.530	0.033	6.31	0.24	6.34	0.19	99.6	4.8
60.58	0.9	0.9058	0.0029	0.530	0.032	6.30	0.24	6.32	0.19	99.7	4.9
75.75	0.9	0.9064	0.0028	0.536	0.031	6.36	0.22	6.36	0.19	100.1	4.6
75.55	0.9	0.9070	0.0028	0.540	0.031	6.33	0.24	6.35	0.19	99.8	4.8
75.35	0.9	0.9057	0.0029	0.534	0.031	6.43	0.25	6.40	0.19	100.5	4.9
15.27	0.9	0.9481	0.0022	0.488	0.067	3.09	0.11	3.07	0.09	100.7	4.6
15.27	0.9	0.9486	0.0021	0.490	0.068	3.05	0.10	3.06	0.09	99.9	4.5
15.20	0.9	0.9491	0.0021	0.489	0.068	3.06	0.10	3.02	0.09	101.5	4.5
29.50	0.9	0.9464	0.0019	0.499	0.041	3.29	0.09	3.25	0.10	101.1	4.2
29.88	0.9	0.9478	0.0019	0.505	0.041	3.15	0.11	3.20	0.10	98.3	4.5
29.86	0.9	0.9478	0.0019	0.503	0.041	3.19	0.11	3.19	0.10	100.1	4.5
44.56	0.9	0.9508	0.0017	0.524	0.035	3.13	0.10	3.12	0.09	100.2	4.5
44.69	0.9	0.9512	0.0016	0.525	0.035	3.09	0.10	3.10	0.09	99.8	4.5
44.67	0.9	0.9511	0.0017	0.522	0.035	3.11	0.10	3.08	0.09	100.9	4.5
60.03	0.9	0.9546	0.0015	0.545	0.034	2.93	0.09	2.98	0.09	98.3	4.3
60.25	0.9	0.9510	0.0016	0.482	0.030	2.83	0.09	2.86	0.09	99.0	4.4
59.93	0.9	0.9514	0.0016	0.485	0.030	2.87	0.08	2.85	0.09	100.7	4.2
75.14	0.9	0.9560	0.0014	0.562	0.033	2.95	0.09	2.98	0.09	99.2	4.3
74.90	0.9	0.9558	0.0014	0.561	0.033	2.99	0.06	2.98	0.09	100.3	3.7
74.86	0.9	0.9467	0.0017	0.449	0.026	2.95	0.06	2.91	0.09	101.2	3.7
16.19	0.9	0.8976	0.0034	0.975	0.127	12.47	0.72	12.78	0.26	97.6	6.0
15.75	0.9	0.8971	0.0035	0.968	0.130	13.02	0.90	12.76	0.26	102.1	7.4
15.77	0.9	0.8976	0.0034	0.970	0.130	12.53	0.70	12.72	0.26	98.5	5.9

31.05	0.9	0.9004	0.0027	1.038	0.083	12.97	0.59	13.19	0.27	98.3	4.9
30.78	0.9	0.9036	0.0026	1.049	0.084	12.65	0.65	12.87	0.26	98.3	5.4
30.64	0.9	0.9037	0.0026	1.047	0.084	12.80	0.61	12.83	0.26	99.7	5.2
45.47	0.9	0.9074	0.0023	1.074	0.072	12.50	0.65	12.58	0.25	99.4	5.5
46.26	0.9	0.9047	0.0024	1.082	0.072	12.88	0.68	13.08	0.26	98.5	5.5
46.11	0.9	0.9065	0.0023	1.070	0.071	12.40	0.70	12.69	0.26	97.8	5.9
61.11	0.9	0.9007	0.0023	1.001	0.061	12.52	0.60	12.64	0.26	99.1	5.2
60.98	0.9	0.9005	0.0023	0.998	0.061	12.69	0.57	12.63	0.26	100.4	4.9
61.10	0.9	0.9000	0.0023	0.992	0.061	12.46	0.72	12.64	0.26	98.5	6.0
75.68	0.9	0.9003	0.0023	1.009	0.059	12.71	0.60	12.82	0.26	99.1	5.1
75.85	0.9	0.9024	0.0022	1.041	0.060	12.49	0.62	12.87	0.26	97.1	5.2
75.92	0.9	0.8997	0.0023	1.008	0.058	12.74	0.66	12.88	0.26	99.0	5.5
15.19	0.9	0.9510	0.0020	1.035	0.144	6.16	0.21	6.13	0.18	100.5	4.5
15.08	0.9	0.9508	0.0021	1.033	0.145	6.21	0.21	6.15	0.18	101.0	4.6
15.06	0.9	0.9510	0.0021	1.033	0.145	6.20	0.20	6.12	0.18	101.4	4.5
30.30	0.9	0.9482	0.0019	0.985	0.080	6.29	0.24	6.20	0.19	101.5	4.9
30.54	0.9	0.9480	0.0019	0.989	0.079	6.28	0.23	6.24	0.19	100.6	4.8
30.46	0.9	0.9475	0.0019	0.986	0.079	6.34	0.20	6.28	0.19	100.9	4.4
45.63	0.9	0.9494	0.0017	1.030	0.069	6.36	0.21	6.32	0.19	100.6	4.5
45.77	0.9	0.9487	0.0017	1.024	0.069	6.39	0.22	6.37	0.19	100.4	4.6
45.77	0.9	0.9485	0.0017	1.025	0.069	6.47	0.22	6.39	0.19	101.2	4.6
60.78	0.9	0.9521	0.0016	1.039	0.064	6.10	0.20	6.02	0.18	101.4	4.6
60.89	0.9	0.9518	0.0016	1.036	0.064	6.10	0.21	6.03	0.18	101.1	4.6
60.91	0.9	0.9519	0.0016	1.043	0.064	6.14	0.19	6.06	0.18	101.4	4.4
75.90	0.9	0.9525	0.0015	1.039	0.060	6.01	0.21	5.96	0.18	100.9	4.7
75.97	0.9	0.9523	0.0015	1.038	0.060	6.06	0.20	5.98	0.18	101.4	4.5
75.43	0.9	0.9521	0.0015	1.040	0.061	6.11	0.19	6.02	0.18	101.6	4.4
15.31	0.9	0.9499	0.0018	1.484	0.205	9.11	0.39	9.01	0.18	101.1	4.8
15.54	0.9	0.9496	0.0018	1.485	0.202	8.89	0.35	9.07	0.18	98.0	4.3
15.26	0.9	0.9492	0.0018	1.477	0.205	9.05	0.39	9.11	0.18	99.3	4.8
30.60	0.9	0.9505	0.0014	1.535	0.123	9.29	0.39	9.21	0.19	100.9	4.7
30.46	0.9	0.9503	0.0014	1.532	0.123	9.27	0.36	9.22	0.19	100.6	4.4
30.45	0.9	0.9507	0.0014	1.537	0.124	9.27	0.41	9.18	0.19	101.0	4.9
45.70	0.9	0.9521	0.0013	1.585	0.106	9.18	0.45	9.18	0.19	99.9	5.3
45.64	0.9	0.9524	0.0012	1.583	0.106	9.13	0.40	9.11	0.18	100.2	4.9
45.63	0.9	0.9528	0.0012	1.587	0.106	9.10	0.40	9.04	0.18	100.6	4.9
60.13	0.9	0.9490	0.0013	1.452	0.089	9.15	0.39	8.97	0.18	102.0	4.8
60.50	0.9	0.9494	0.0013	1.463	0.090	9.07	0.38	8.97	0.18	101.2	4.7
60.33	0.9	0.9475	0.0013	1.454	0.089	9.45	0.40	9.27	0.19	101.9	4.8

74.34	0.9	0.9497	0.0012	1.475	0.086	9.12	0.30	8.99	0.18	101.5	3.9
75.33	0.9	0.9501	0.0012	1.472	0.086	8.94	0.39	8.89	0.18	100.6	4.9
75.27	0.9	0.9503	0.0012	1.479	0.086	9.02	0.37	8.90	0.18	101.3	4.6
15.18	0.9	0.9493	0.0018	1.973	0.275	12.01	0.57	12.11	0.24	99.1	5.1
15.45	0.9	0.9495	0.0018	1.983	0.271	12.14	0.68	12.12	0.25	100.2	5.9
15.11	0.9	0.9494	0.0018	1.976	0.277	12.15	0.78	12.13	0.25	100.2	6.8
30.02	0.9	0.9486	0.0015	1.938	0.157	12.14	0.69	12.09	0.24	100.5	6.1
30.06	0.9	0.9476	0.0015	1.906	0.155	12.04	0.58	12.12	0.25	99.3	5.2
30.05	0.9	0.9481	0.0015	1.924	0.156	11.99	0.52	12.12	0.25	99.0	4.7
44.68	0.9	0.9496	0.0013	1.967	0.133	12.08	0.53	12.00	0.24	100.7	4.9
45.12	0.9	0.9505	0.0013	1.995	0.134	12.13	0.65	11.97	0.24	101.3	5.8
45.11	0.9	0.9505	0.0013	2.002	0.135	12.04	0.65	11.99	0.24	100.4	5.8
59.94	0.9	0.9506	0.0012	1.998	0.123	11.74	0.54	11.94	0.24	98.3	4.9
60.18	0.9	0.9506	0.0012	2.006	0.123	11.68	0.61	11.98	0.24	97.5	5.5
60.18	0.9	0.9514	0.0012	2.032	0.125	11.74	0.47	11.95	0.24	98.3	4.4
74.68	0.9	0.9513	0.0012	2.016	0.118	11.33	0.52	11.87	0.24	95.4	4.8
75.09	0.9	0.9497	0.0012	2.027	0.118	11.85	0.73	12.35	0.25	96.0	6.2
75.16	0.9	0.9499	0.0012	2.012	0.117	11.76	0.60	12.21	0.25	96.3	5.3
15.18	0.9	0.9481	0.0019	2.465	0.343	15.16	0.84	15.52	0.31	97.7	5.8
15.20	0.9	0.9484	0.0019	2.465	0.343	15.23	0.84	15.43	0.31	98.7	5.8
15.17	0.9	0.9487	0.0018	2.462	0.343	14.81	0.82	15.33	0.31	96.6	5.7
15.17	0.9	0.9487	0.0018	2.460	0.343	15.12	0.86	15.33	0.31	98.6	6.0
30.40	0.9	0.9487	0.0015	2.432	0.196	15.12	0.93	15.12	0.31	100.0	6.5
30.25	0.9	0.9510	0.0014	2.563	0.207	15.01	0.75	15.18	0.31	98.9	5.3
30.31	0.9	0.9515	0.0014	2.591	0.209	15.00	0.91	15.18	0.31	98.8	6.3
45.09	0.9	0.9503	0.0013	2.474	0.167	15.10	0.80	14.90	0.30	101.3	5.8
45.73	0.9	0.9501	0.0013	2.492	0.167	14.85	1.00	15.06	0.30	98.6	6.9
45.77	0.9	0.9505	0.0013	2.505	0.168	14.64	0.88	15.01	0.30	97.6	6.2
59.89	0.9	0.9498	0.0012	2.497	0.154	14.69	0.95	15.19	0.31	96.7	6.6
60.57	0.9	0.9503	0.0012	2.517	0.154	14.60	0.80	15.15	0.31	96.4	5.7
60.57	0.9	0.9502	0.0012	2.514	0.154	14.83	0.82	15.14	0.31	97.9	5.8
76.02	0.9	0.9501	0.0012	2.516	0.146	15.01	1.00	15.21	0.31	98.7	6.9
76.33	0.9	0.9502	0.0012	2.506	0.145	14.95	0.88	15.08	0.30	99.1	6.2
76.27	0.9	0.9494	0.0012	2.494	0.145	15.18	0.95	15.26	0.31	99.5	6.6
15.03	0.9	0.9899	0.0004	2.506	0.353	2.95	0.07	2.95	0.09	100.1	3.9
14.98	0.9	0.9899	0.0004	2.505	0.354	2.95	0.08	2.95	0.09	100.1	4.0
14.98	0.9	0.9899	0.0004	2.504	0.354	2.96	0.07	2.95	0.09	100.4	3.9
30.14	0.9	0.9897	0.0004	2.529	0.205	3.03	0.07	3.02	0.09	100.2	3.7
30.10	0.9	0.9897	0.0004	2.528	0.205	3.03	0.07	3.02	0.09	100.1	3.8

30.09	0.9	0.9897	0.0004	2.530	0.205	3.03	0.07	3.03	0.09	100.1	3.8
44.91	0.9	0.9892	0.0004	2.560	0.173	3.22	0.08	3.22	0.10	100.2	3.9
45.23	0.9	0.9891	0.0004	2.550	0.172	3.25	0.07	3.24	0.10	100.6	3.7
45.23	0.9	0.9891	0.0004	2.556	0.172	3.26	0.07	3.23	0.10	100.9	3.8
65.18	0.9	0.9892	0.0004	2.562	0.155	3.24	0.08	3.23	0.10	100.4	3.9
65.20	0.9	0.9891	0.0004	2.561	0.154	3.28	0.08	3.26	0.10	100.5	3.9
65.16	0.9	0.9890	0.0004	2.563	0.155	3.31	0.08	3.27	0.10	101.1	3.9
75.05	0.9	0.9898	0.0003	2.468	0.144	2.95	0.07	2.94	0.09	100.4	3.8
75.07	0.9	0.9898	0.0003	2.467	0.144	2.94	0.07	2.92	0.09	100.7	3.8
75.15	0.9	0.9899	0.0003	2.465	0.144	2.92	0.06	2.90	0.09	100.6	3.8

Table D.2. 4" Tee Results

Pressure (psi)	dP	GVF	dGVF	Velocity (m/s)	dV	dV/dt (GPM)	d(dV/dt)	Qi (GPM)	dQi	η (%)	dη
15.09	0.9	0.8912	0.0043	0.468	0.065	6.59	0.27	6.55	0.20	100.6	5.2
15.29	0.9	0.8931	0.0042	0.471	0.065	6.50	0.21	6.47	0.19	100.5	4.4
15.35	0.9	0.8971	0.0041	0.480	0.066	6.31	0.23	6.31	0.19	99.9	4.7
30.38	0.9	0.8974	0.0035	0.487	0.039	6.42	0.26	6.39	0.19	100.4	5.1
30.68	0.9	0.8980	0.0035	0.490	0.039	6.38	0.23	6.38	0.19	100.0	4.7
30.71	0.9	0.8980	0.0035	0.490	0.039	6.36	0.23	6.39	0.19	99.6	4.7
45.76	0.9	0.8991	0.0032	0.508	0.034	6.55	0.23	6.54	0.20	100.0	4.6
45.91	0.9	0.8983	0.0032	0.508	0.034	6.63	0.25	6.60	0.20	100.3	4.8
45.80	0.9	0.9024	0.0031	0.514	0.034	6.36	0.24	6.38	0.19	99.8	4.8
60.70	0.9	0.9039	0.0030	0.519	0.032	6.40	0.25	6.34	0.19	100.9	5.0
60.53	0.9	0.9039	0.0030	0.519	0.032	6.39	0.18	6.34	0.19	100.7	4.2
60.11	0.9	0.9038	0.0030	0.519	0.032	6.36	0.23	6.35	0.19	100.3	4.8
75.31	0.9	0.9061	0.0029	0.529	0.031	6.38	0.22	6.30	0.19	101.3	4.6
75.37	0.9	0.9071	0.0028	0.532	0.031	6.29	0.21	6.26	0.19	100.6	4.5
75.33	0.9	0.9063	0.0029	0.527	0.031	6.29	0.22	6.26	0.19	100.4	4.6
14.82	0.9	0.9564	0.0018	0.564	0.081	2.98	0.07	2.96	0.09	100.9	3.8
14.44	0.9	0.9544	0.0019	0.561	0.082	3.07	0.07	3.08	0.09	99.5	3.7
14.84	0.9	0.9480	0.0022	0.495	0.071	3.14	0.08	3.13	0.09	100.2	3.9
29.97	0.9	0.9507	0.0018	0.515	0.042	3.04	0.07	3.08	0.09	99.0	3.8
30.01	0.9	0.9509	0.0018	0.514	0.042	3.01	0.07	3.05	0.09	98.7	3.8
30.01	0.9	0.9512	0.0018	0.515	0.042	3.01	0.06	3.04	0.09	98.9	3.6
44.78	0.9	0.9544	0.0015	0.535	0.036	2.93	0.07	2.94	0.09	99.6	3.9
44.92	0.9	0.9547	0.0015	0.536	0.036	2.92	0.07	2.93	0.09	99.7	3.8

44.97	0.9	0.9507	0.0017	0.534	0.036	3.14	0.08	3.19	0.10	98.6	3.8
59.97	0.9	0.9527	0.0015	0.546	0.034	3.10	0.06	3.12	0.09	99.3	3.5
60.04	0.9	0.9522	0.0016	0.545	0.034	3.14	0.07	3.15	0.09	99.6	3.8
59.96	0.9	0.9519	0.0016	0.546	0.034	3.17	0.07	3.17	0.10	99.9	3.8
75.15	0.9	0.9554	0.0014	0.554	0.032	2.97	0.07	2.98	0.09	99.7	3.7
75.12	0.9	0.9513	0.0016	0.552	0.032	3.23	0.07	3.25	0.10	99.5	3.8
75.52	0.9	0.9553	0.0014	0.555	0.032	2.96	0.06	2.99	0.09	99.2	3.6
15.02	0.9	0.9034	0.0033	1.046	0.147	12.75	0.70	12.86	0.26	99.2	5.8
15.14	0.9	0.9031	0.0033	1.043	0.145	13.02	0.66	12.86	0.26	101.3	5.5
15.21	0.9	0.9055	0.0032	1.072	0.149	12.86	0.69	12.85	0.26	100.1	5.7
30.64	0.9	0.8996	0.0027	0.995	0.080	12.62	0.69	12.76	0.26	99.0	5.8
30.80	0.9	0.8994	0.0027	0.996	0.079	12.96	0.61	12.76	0.26	101.6	5.2
30.71	0.9	0.8975	0.0028	0.975	0.078	12.86	0.69	12.78	0.26	100.7	5.8
45.87	0.9	0.9040	0.0024	1.065	0.071	12.89	0.46	13.00	0.26	99.2	4.1
46.26	0.9	0.9016	0.0024	1.038	0.069	13.03	0.45	13.02	0.26	100.1	4.0
46.35	0.9	0.9011	0.0024	1.037	0.069	13.10	0.72	13.05	0.26	100.4	5.9
61.76	0.9	0.9076	0.0022	1.079	0.066	12.32	0.66	12.61	0.25	97.7	5.6
61.70	0.9	0.9087	0.0022	1.092	0.067	12.15	0.47	12.60	0.25	96.4	4.2
61.74	0.9	0.9005	0.0023	1.010	0.062	12.54	0.55	12.80	0.26	97.9	4.7
76.16	0.9	0.9025	0.0022	1.008	0.059	12.68	0.66	12.50	0.25	101.5	5.7
76.98	0.9	0.9052	0.0022	1.037	0.060	12.30	0.61	12.46	0.25	98.7	5.3
76.41	0.9	0.9016	0.0022	1.001	0.058	12.31	0.42	12.52	0.25	98.3	3.9
15.11	0.9	0.9484	0.0022	0.989	0.138	6.26	0.19	6.19	0.19	101.1	4.4
15.27	0.9	0.9489	0.0021	0.994	0.138	6.17	0.20	6.16	0.19	100.2	4.5
15.13	0.9	0.9484	0.0022	0.989	0.138	6.28	0.21	6.20	0.19	101.4	4.6
29.89	0.9	0.9482	0.0019	0.969	0.079	6.20	0.22	6.09	0.18	101.9	4.8
30.35	0.9	0.9490	0.0018	0.969	0.078	6.07	0.18	5.99	0.18	101.3	4.3
29.79	0.9	0.9488	0.0018	0.967	0.079	6.17	0.21	6.01	0.18	102.7	4.6
44.96	0.9	0.9508	0.0017	0.999	0.067	6.08	0.21	5.95	0.18	102.3	4.7
45.03	0.9	0.9509	0.0017	1.001	0.067	6.01	0.20	5.94	0.18	101.3	4.6
45.12	0.9	0.9511	0.0016	1.004	0.068	6.02	0.18	5.93	0.18	101.4	4.3
60.18	0.9	0.9518	0.0016	1.013	0.062	5.98	0.16	5.90	0.18	101.4	4.1
60.27	0.9	0.9523	0.0016	1.021	0.063	5.97	0.18	5.88	0.18	101.4	4.3
60.24	0.9	0.9523	0.0016	1.020	0.063	5.95	0.17	5.88	0.18	101.2	4.2
75.01	0.9	0.9509	0.0016	1.020	0.060	6.17	0.21	6.06	0.18	101.8	4.6
75.42	0.9	0.9509	0.0016	1.021	0.059	6.18	0.17	6.07	0.18	101.8	4.1
75.45	0.9	0.9509	0.0016	1.020	0.059	6.12	0.18	6.06	0.18	101.0	4.3
15.25	0.9	0.9497	0.0018	1.505	0.208	9.08	0.42	9.18	0.19	99.0	5.0
15.50	0.9	0.9485	0.0018	1.443	0.197	8.61	0.34	9.02	0.18	95.5	4.3

15.79	0.9	0.9488	0.0018	1.503	0.201	9.32	0.39	9.34	0.19	99.7	4.7
30.66	0.9	0.9504	0.0014	1.533	0.123	9.16	0.40	9.19	0.19	99.6	4.8
30.11	0.9	0.9520	0.0014	1.555	0.126	9.06	0.46	9.03	0.18	100.3	5.5
30.10	0.9	0.9513	0.0014	1.536	0.124	9.05	0.39	9.04	0.18	100.1	4.8
44.93	0.9	0.9466	0.0014	1.450	0.098	9.52	0.37	9.40	0.19	101.2	4.5
45.18	0.9	0.9509	0.0013	1.508	0.102	9.10	0.39	8.97	0.18	101.5	4.8
45.45	0.9	0.9511	0.0013	1.529	0.103	9.17	0.36	9.04	0.18	101.4	4.5
60.40	0.9	0.9517	0.0012	1.538	0.095	9.05	0.47	8.98	0.18	100.8	5.6
60.42	0.9	0.9516	0.0012	1.553	0.095	9.21	0.36	9.08	0.18	101.5	4.5
60.45	0.9	0.9514	0.0012	1.556	0.096	9.18	0.38	9.14	0.19	100.5	4.6
75.18	0.9	0.9522	0.0011	1.575	0.092	9.01	0.36	9.09	0.18	99.1	4.5
75.16	0.9	0.9524	0.0011	1.566	0.091	8.90	0.36	9.00	0.18	98.8	4.5
75.17	0.9	0.9525	0.0011	1.560	0.091	8.82	0.39	8.95	0.18	98.6	4.8
14.66	0.9	0.9486	0.0019	1.938	0.280	12.05	0.61	12.07	0.24	99.8	5.5
15.36	0.9	0.9502	0.0018	2.039	0.280	12.20	0.72	12.30	0.25	99.2	6.2
15.36	0.9	0.9500	0.0018	2.033	0.280	12.34	0.59	12.31	0.25	100.2	5.2
30.19	0.9	0.9493	0.0015	1.963	0.159	12.07	0.57	12.06	0.24	100.1	5.1
30.51	0.9	0.9498	0.0015	1.985	0.160	12.06	0.52	12.08	0.24	99.9	4.8
30.51	0.9	0.9498	0.0015	1.993	0.160	12.05	0.59	12.10	0.24	99.6	5.3
46.03	0.9	0.9515	0.0013	2.064	0.138	12.04	0.60	12.11	0.24	99.4	5.4
46.05	0.9	0.9511	0.0013	2.048	0.137	12.09	0.64	12.12	0.25	99.8	5.6
45.81	0.9	0.9508	0.0013	2.041	0.137	12.12	0.65	12.15	0.25	99.7	5.7
60.58	0.9	0.9515	0.0012	2.095	0.129	12.27	0.64	12.28	0.25	99.9	5.6
60.70	0.9	0.9510	0.0012	2.076	0.127	12.24	0.66	12.32	0.25	99.4	5.7
60.75	0.9	0.9507	0.0012	2.058	0.126	12.40	0.58	12.28	0.25	101.0	5.1
75.05	0.9	0.9521	0.0011	2.091	0.122	11.92	0.56	12.10	0.24	98.5	5.0
75.03	0.9	0.9513	0.0012	2.053	0.120	11.90	0.64	12.07	0.24	98.6	5.6
74.70	0.9	0.9513	0.0012	2.047	0.120	11.64	0.58	12.06	0.24	96.6	5.2
15.57	0.9	0.9456	0.0019	2.355	0.320	15.67	0.84	15.60	0.31	100.5	5.8
15.18	0.9	0.9503	0.0018	2.516	0.350	15.29	0.84	15.13	0.31	101.1	5.9
15.56	0.9	0.9507	0.0018	2.535	0.344	15.09	0.77	15.11	0.30	99.8	5.5
29.98	0.9	0.9494	0.0015	2.505	0.203	15.33	1.00	15.36	0.31	99.8	6.8
30.46	0.9	0.9498	0.0015	2.522	0.203	15.04	0.79	15.32	0.31	98.1	5.5
30.42	0.9	0.9501	0.0014	2.518	0.203	15.00	0.66	15.22	0.31	98.6	4.8
45.05	0.9	0.9525	0.0012	2.619	0.176	14.54	0.95	15.01	0.30	96.8	6.6
44.56	0.9	0.9515	0.0013	2.567	0.174	14.42	1.09	15.07	0.30	95.7	7.5
44.72	0.9	0.9525	0.0012	2.617	0.177	14.64	0.88	15.00	0.30	97.6	6.2
59.42	0.9	0.9488	0.0013	2.469	0.152	15.08	0.88	15.32	0.31	98.4	6.1
59.98	0.9	0.9509	0.0012	2.539	0.156	14.98	0.80	15.09	0.30	99.3	5.7

59.19	0.9	0.9494	0.0013	2.518	0.155	14.96	1.12	15.40	0.31	97.2	7.5
14.96	0.9	0.9901	0.0004	2.523	0.357	2.92	0.07	2.90	0.09	100.7	3.8
14.90	0.9	0.9900	0.0004	2.515	0.357	2.96	0.06	2.92	0.09	101.2	3.8
14.95	0.9	0.9902	0.0004	2.522	0.357	2.92	0.06	2.88	0.09	101.3	3.8
30.07	0.9	0.9898	0.0004	2.487	0.202	2.98	0.07	2.95	0.09	100.9	3.9
30.05	0.9	0.9898	0.0004	2.486	0.202	2.98	0.07	2.94	0.09	101.1	3.9
30.07	0.9	0.9899	0.0004	2.489	0.202	2.97	0.07	2.93	0.09	101.2	3.9
44.69	0.9	0.9900	0.0004	2.509	0.170	2.92	0.07	2.91	0.09	100.3	3.8
45.25	0.9	0.9900	0.0003	2.518	0.169	2.95	0.07	2.92	0.09	100.9	3.9
45.17	0.9	0.9900	0.0004	2.518	0.170	2.96	0.07	2.94	0.09	100.6	3.9
59.66	0.9	0.9900	0.0003	2.514	0.155	2.93	0.07	2.93	0.09	100.0	3.9
60.21	0.9	0.9899	0.0003	2.516	0.155	2.98	0.07	2.96	0.09	100.5	3.8
60.23	0.9	0.9898	0.0003	2.515	0.155	3.00	0.07	2.97	0.09	100.9	3.9
75.01	0.9	0.9896	0.0003	2.415	0.141	2.95	0.06	2.93	0.09	100.5	3.6
75.11	0.9	0.9895	0.0003	2.494	0.146	3.03	0.07	3.04	0.09	99.9	3.8
74.96	0.9	0.9896	0.0003	2.490	0.145	3.04	0.06	3.02	0.09	100.5	3.5

Table D.3. 6" Wye Results

Pressure (psi)	dP	GVF	dGVF	Velocity (m/s)	dV	dV/dt (GPM)	d(dV/dt)	Qi (GPM)	dQi	η (%)	dη
15.68	0.90	0.9013	0.0034	0.515	0.024	14.44	0.31	14.51	0.29	99.5	2.9
15.83	0.90	0.9002	0.0005	0.517	0.183	14.59	0.21	14.70	0.30	99.3	2.4
15.66	0.90	0.9016	0.0005	0.515	0.183	14.43	0.20	14.45	0.29	99.8	2.4
30.95	0.90	0.9034	0.0004	0.516	0.162	14.10	0.20	14.19	0.29	99.4	2.5
31.01	0.90	0.9030	0.0004	0.517	0.162	14.27	0.21	14.25	0.29	100.1	2.5
30.99	0.90	0.9031	0.0004	0.514	0.161	14.14	0.21	14.17	0.29	99.8	2.5
46.08	0.90	0.9049	0.0004	0.533	0.159	14.47	0.19	14.39	0.29	100.6	2.4
46.05	0.90	0.9044	0.0004	0.532	0.159	14.52	0.21	14.45	0.29	100.5	2.5
46.24	0.90	0.9077	0.0004	0.535	0.159	13.94	0.17	13.97	0.28	99.7	2.4
61.69	0.90	0.8984	0.0004	0.488	0.142	14.14	0.18	14.17	0.29	99.8	2.4
61.05	0.90	0.8958	0.0004	0.471	0.137	14.12	0.20	14.09	0.28	100.2	2.5
61.57	0.90	0.8995	0.0004	0.493	0.143	14.17	0.19	14.16	0.29	100.1	2.4
76.28	0.90	0.9002	0.0004	0.480	0.137	13.62	0.18	13.67	0.28	99.7	2.4
76.76	0.90	0.8932	0.0004	0.480	0.137	14.69	0.20	14.75	0.30	99.6	2.4
77.34	0.90	0.8935	0.0004	0.480	0.137	14.62	0.20	14.68	0.30	99.5	2.4
32.49	0.90	0.9045	0.0004	1.048	0.326	28.19	0.64	28.45	0.57	99.1	3.0
32.30	0.90	0.9041	0.0004	1.044	0.325	28.36	0.56	28.48	0.57	99.6	2.8

30.81	0.90	0.9032	0.0004	1.044	0.328	29.05	0.67	28.75	0.58	101.0	3.1
46.24	0.90	0.8953	0.0004	0.942	0.281	28.41	0.71	28.33	0.57	100.3	3.2
46.10	0.90	0.8965	0.0004	0.954	0.285	27.83	0.59	28.32	0.57	98.3	2.9
45.57	0.90	0.8963	0.0004	0.957	0.286	28.32	0.60	28.46	0.57	99.5	2.9
60.61	0.90	0.9034	0.0004	0.962	0.280	25.81	0.48	26.43	0.53	97.7	2.7
61.52	0.90	0.8968	0.0004	0.947	0.275	27.24	0.61	28.03	0.56	97.2	2.9
61.22	0.90	0.8984	0.0004	0.961	0.279	27.28	0.59	27.93	0.56	97.7	2.9
76.44	0.90	0.9000	0.0004	0.975	0.279	26.35	0.56	27.83	0.56	94.7	2.8
76.49	0.90	0.8986	0.0004	0.959	0.275	26.74	0.55	27.84	0.56	96.1	2.8
76.47	0.90	0.8991	0.0004	0.966	0.277	26.59	0.58	27.85	0.56	95.5	2.8
15.07	0.90	0.9516	0.0003	0.517	0.185	6.77	0.07	6.76	0.20	100.2	3.2
15.30	0.90	0.9509	0.0003	0.518	0.185	6.97	0.07	6.88	0.21	101.3	3.2
15.06	0.90	0.9530	0.0003	0.518	0.185	6.66	0.07	6.57	0.20	101.3	3.2
30.33	0.90	0.9490	0.0003	0.496	0.156	6.86	0.06	6.85	0.21	100.1	3.1
30.20	0.90	0.9509	0.0003	0.496	0.156	6.65	0.06	6.59	0.20	101.0	3.2
30.22	0.90	0.9502	0.0003	0.495	0.156	6.71	0.07	6.67	0.20	100.6	3.2
45.19	0.90	0.9513	0.0002	0.512	0.153	6.77	0.07	6.74	0.20	100.4	3.2
45.20	0.90	0.9474	0.0003	0.510	0.152	7.35	0.08	7.27	0.22	101.1	3.2
45.57	0.90	0.9509	0.0002	0.511	0.153	6.83	0.07	6.79	0.20	100.6	3.2
60.69	0.90	0.9522	0.0002	0.539	0.157	7.00	0.08	6.96	0.21	100.5	3.2
60.71	0.90	0.9531	0.0002	0.542	0.158	6.89	0.07	6.86	0.21	100.5	3.2
60.62	0.90	0.9520	0.0002	0.537	0.156	7.02	0.07	6.97	0.21	100.7	3.2
75.92	0.90	0.9508	0.0002	0.504	0.145	6.73	0.06	6.71	0.20	100.3	3.1
75.37	0.90	0.9507	0.0002	0.501	0.144	6.70	0.07	6.68	0.20	100.3	3.2
75.60	0.90	0.9509	0.0002	0.503	0.144	6.72	0.06	6.70	0.20	100.4	3.2
15.33	0.90	0.9494	0.0003	0.981	0.350	13.57	0.19	13.44	0.27	101.0	2.5
15.38	0.90	0.9492	0.0003	0.980	0.349	13.64	0.19	13.49	0.27	101.1	2.5
15.46	0.90	0.9495	0.0003	0.982	0.349	13.54	0.20	13.42	0.27	100.8	2.5
30.55	0.90	0.9497	0.0002	0.978	0.308	13.46	0.18	13.33	0.27	101.0	2.5
30.85	0.90	0.9498	0.0002	0.982	0.308	13.45	0.20	13.36	0.27	100.7	2.5
30.37	0.90	0.9499	0.0002	0.979	0.308	13.38	0.19	13.29	0.27	100.6	2.5
45.53	0.90	0.9499	0.0002	0.993	0.297	13.55	0.17	13.48	0.27	100.5	2.4
45.93	0.90	0.9501	0.0002	0.996	0.298	13.53	0.22	13.46	0.27	100.5	2.6
45.53	0.90	0.9527	0.0002	1.075	0.315	13.59	0.17	13.48	0.27	100.8	2.4
60.61	0.90	0.9498	0.0002	1.001	0.292	13.61	0.19	13.61	0.27	100.0	2.5
60.18	0.90	0.9508	0.0002	1.004	0.293	13.33	0.20	13.38	0.27	99.7	2.5
60.58	0.90	0.9512	0.0002	1.011	0.295	13.37	0.19	13.36	0.27	100.0	2.5
75.23	0.90	0.9510	0.0002	1.014	0.291	13.40	0.18	13.43	0.27	99.8	2.4
75.02	0.90	0.9491	0.0002	1.007	0.289	13.84	0.21	13.92	0.28	99.4	2.5

75.32	0.90	0.9503	0.0002	1.008	0.290	13.55	0.20	13.56	0.27	99.9	2.5
15.23	0.90	0.9455	0.0003	1.456	0.519	21.90	0.39	21.59	0.43	101.5	2.7
15.27	0.90	0.9458	0.0003	1.458	0.520	21.68	0.43	21.50	0.43	100.8	2.8
15.58	0.90	0.9462	0.0003	1.465	0.520	21.54	0.37	21.41	0.43	100.6	2.7
30.32	0.90	0.9499	0.0002	1.512	0.476	20.46	0.33	20.51	0.41	99.8	2.6
30.27	0.90	0.9498	0.0002	1.512	0.476	20.47	0.32	20.55	0.41	99.6	2.5
30.85	0.90	0.9503	0.0002	1.515	0.476	20.26	0.32	20.38	0.41	99.4	2.5
45.52	0.90	0.9496	0.0002	1.488	0.445	19.96	0.32	20.35	0.41	98.1	2.5
46.01	0.90	0.9501	0.0002	1.500	0.448	19.99	0.36	20.26	0.41	98.7	2.7
44.31	0.90	0.9488	0.0002	1.471	0.441	20.16	0.34	20.42	0.41	98.7	2.6
60.76	0.90	0.9503	0.0002	1.511	0.440	20.18	0.54	20.33	0.41	99.3	3.3
60.50	0.90	0.9502	0.0002	1.512	0.441	20.06	0.36	20.38	0.41	98.5	2.7
60.62	0.90	0.9499	0.0002	1.495	0.435	19.88	0.35	20.31	0.41	97.9	2.6
75.34	0.90	0.9507	0.0002	1.515	0.435	19.81	0.36	20.23	0.41	97.9	2.6
75.42	0.90	0.9498	0.0002	1.518	0.436	20.23	0.38	20.67	0.42	97.9	2.7
74.92	0.90	0.9508	0.0002	1.513	0.434	19.68	0.29	20.13	0.41	97.7	2.5
31.54	0.90	0.9508	0.0002	2.052	0.642	27.51	0.56	27.31	0.55	100.7	2.9
30.45	0.90	0.9494	0.0002	2.014	0.633	27.67	0.55	27.58	0.55	100.3	2.8
30.40	0.90	0.9499	0.0002	2.038	0.641	27.81	0.63	27.61	0.55	100.7	3.0
45.26	0.90	0.9523	0.0002	2.066	0.617	25.74	0.42	26.58	0.53	96.8	2.5
45.70	0.90	0.9516	0.0002	2.081	0.621	26.67	0.48	27.19	0.55	98.1	2.6
45.68	0.90	0.9514	0.0002	2.064	0.616	26.00	0.46	27.07	0.54	96.0	2.6
60.73	0.90	0.9526	0.0002	2.096	0.610	25.78	0.54	26.79	0.54	96.2	2.8
60.91	0.90	0.9517	0.0002	2.096	0.610	26.53	0.55	27.35	0.55	97.0	2.8
60.89	0.90	0.9522	0.0002	2.100	0.611	26.35	0.56	27.12	0.55	97.2	2.8
74.75	0.90	0.9517	0.0002	2.054	0.589	25.38	0.56	26.83	0.54	94.6	2.8
74.78	0.90	0.9517	0.0002	2.052	0.589	25.55	0.58	26.80	0.54	95.3	2.9
74.69	0.90	0.9521	0.0002	2.050	0.588	24.80	0.58	26.50	0.53	93.6	2.9
15.05	0.90	0.9905	0.0001	2.568	0.919	6.49	0.05	6.33	0.19	102.6	3.2
15.06	0.90	0.9903	0.0001	2.576	0.921	6.35	0.05	6.48	0.19	97.9	3.0
15.07	0.90	0.9902	0.0001	2.568	0.919	6.70	0.05	6.55	0.20	102.3	3.2
30.19	0.90	0.9900	0.0001	2.529	0.797	6.59	0.05	6.58	0.20	100.2	3.1
30.14	0.90	0.9902	0.0001	2.543	0.802	6.53	0.07	6.51	0.20	100.4	3.2
30.13	0.90	0.9902	0.0000	2.530	0.798	6.52	0.05	6.45	0.19	101.0	3.1
44.13	0.90	0.9902	0.0000	2.564	0.769	6.51	0.08	6.51	0.20	100.1	3.3
45.22	0.90	0.9904	0.0000	2.578	0.771	6.50	0.05	6.46	0.19	100.5	3.1
45.15	0.90	0.9902	0.0000	2.560	0.766	6.55	0.05	6.49	0.19	101.0	3.1
65.28	0.90	0.9904	0.0000	2.584	0.748	6.47	0.06	6.43	0.19	100.7	3.2
65.30	0.90	0.9904	0.0000	2.585	0.749	6.45	0.07	6.44	0.19	100.2	3.2

65.20	0.90	0.9904	0.0000	2.589	0.750	6.51	0.05	6.45	0.19	100.9	3.1
75.14	0.90	0.9901	0.0000	2.521	0.724	6.50	0.07	6.49	0.20	100.2	3.2
75.38	0.90	0.9901	0.0000	2.519	0.723	6.49	0.06	6.48	0.19	100.1	3.2
75.16	0.90	0.9901	0.0000	2.525	0.725	6.56	0.07	6.49	0.20	101.1	3.2

Table D.4. Air Entrainment Results

Fitting	Ds in	τ' s/in	dτ'	P (psi)	dP	GVF	dGVF	v m/s	dv	Qw GPM	dQw	LAE (in)	dLAE
wye	3.77	0.48	0.07	60.0	0.9	0.9504	0.0009	1.01	0.06	6.08	0.18	3.2	0.16
wye	3.77	0.23	0.04	60.1	0.9	0.9020	0.0017	1.03	0.06	12.84	0.26	30.4	1.52
wye	3.77	1.65	0.14	60.0	0.9	0.9918	0.0002	1.02	0.10	1.75	0.05	0.5	0.02
wye	3.77	0.31	0.04	29.9	0.9	0.9501	0.0015	1.53	0.10	9.28	0.19	6.1	0.30
wye	3.77	0.32	0.04	44.9	0.9	0.9496	0.0011	1.47	0.09	8.99	0.18	5.8	0.29
wye	3.77	0.32	0.04	60.0	0.9	0.9495	0.0009	1.50	0.09	9.19	0.19	6.8	0.34
wye	3.77	0.32	0.04	74.9	0.9	0.9510	0.0008	1.52	0.09	8.99	0.18	6.0	0.30
wye	3.77	0.23	0.04	59.8	0.9	0.9476	0.0009	1.96	0.11	12.51	0.25	40.9	2.04
tee	3.77	1.44	0.13	61.3	0.9	0.9852	0.0003	0.99	0.07	2.01	0.06	2.1	0.11
tee	3.77	0.48	0.07	60.0	0.9	0.9508	0.0009	1.01	0.06	6.03	0.18	3.0	0.15
tee	3.77	0.23	0.04	59.9	0.9	0.9001	0.0017	1.00	0.06	12.72	0.26	70.6	7.06
tee	3.77	0.33	0.05	30.0	0.9	0.9499	0.0015	1.46	0.09	8.83	0.18	4.4	0.22
tee	3.77	0.32	0.04	44.9	0.9	0.9508	0.0011	1.53	0.09	9.14	0.19	7.9	0.40
tee	3.77	0.31	0.04	60.1	0.9	0.9503	0.0009	1.54	0.09	9.25	0.19	8.8	0.44
tee	3.77	0.32	0.04	75.8	0.9	0.9515	0.0008	1.55	0.09	9.07	0.18	33.2	1.66
tee	3.77	0.23	0.04	60.0	0.9	0.9473	0.0009	1.96	0.11	12.59	0.25	44.1	2.21
wye	5.66	2.49	0.16	60.0	0.9	0.9900	0.0002	1.01	0.04	2.63	0.08	0.7	0.03
wye	5.66	0.48	0.05	60.1	0.9	0.9494	0.0009	1.00	0.04	13.74	0.28	5.5	0.27
wye	5.66	0.23	0.04	60.5	0.9	0.8998	0.0017	0.99	0.04	28.36	0.57	66.0	6.60
wye	5.66	0.33	0.04	30.0	0.9	0.9494	0.0015	1.46	0.07	20.09	0.40	10.1	0.51
wye	5.66	0.32	0.04	45.1	0.9	0.9493	0.0011	1.50	0.06	20.66	0.42	16.3	0.82
wye	5.66	0.33	0.04	59.9	0.9	0.9509	0.0009	1.50	0.06	20.00	0.40	14.7	0.74
wye	5.66	0.33	0.04	75.2	0.9	0.9512	0.0008	1.51	0.06	19.94	0.40	20.4	1.02
wye	5.66	0.24	0.04	60.1	0.9	0.9502	0.0009	2.00	0.08	26.93	0.54	76.4	7.64

VITA

Name: Daniel Ian Cihak

Address: Texas A&M University
Department of Mechanical Engineering
3123 TAMU
College Station, TX, 77843-3123

Email Address: dacihak@gmail.com

Education: B.S., Mechanical Engineering, The University of Texas at Austin, May 2010
M.S., Mechanical Engineering, Texas A&M University, August 2012